

ZEIDAN, EFFAT, Ph.D. Ultra-Sensitive and Multiplex Detection of Clinical Biomarkers Using a SPRi-Based Sensor (2016)  
Directed by Dr. Ethan W. Taylor. 100 pp.

Reliable and reproducible biomarker analysis is the main focus of current clinical diagnostic approaches being developed for the sensitive detection and quantification of biomarkers in bodily fluids. Currently used tools are being revised for better analytical performance that overcomes the drawbacks of inaccurate results. Surface plasmon resonance imaging is rising quickly as an affinity-based optical biosensor that demonstrates numerous improvements to the sensor surface design and sensitivity for label-free and real-time biomarker analysis. In this work, our goal is to develop a more sensitive analytical method for the enhanced detection of the human growth hormone (hGH) in serum, multiplex detection of disease biomarkers (KIM-1 and HMGB-1) simultaneously in buffer using a sandwich-amplification assay, and small molecule-progesterone sensing using a novel aptasensor. Our goals were met by ensuring a homogenous and specific immunosensor for detecting hGH at very low concentrations ( $> 9.1$  pg/mL), substituting random antibody attachment with a site directed immobilization to the sensor surface for multiplex detection of two disease biomarkers down to 5 pg/mL levels in buffer, and further increasing the sensitivity of progesterone biosensor by exploiting x-aptamer technology for highly selective detection of progesterone ( $> 1$  nM) in buffer.

ULTRA-SENSITIVE AND MULTIPLEX DETECTION OF  
CLINICAL BIOMARKERS USING A  
SPRI-BASED SENSOR

by

Effat Zeidan

A Dissertation Submitted to  
the Faculty of the Graduate School at  
The University of North Carolina at Greensboro  
in Partial Fulfillment  
of the Requirements for the Degree  
Doctor of Philosophy

Greensboro  
2016

Approved by

---

Committee Chair

APPROVAL PAGE

This dissertation written by Effat Zeidan has been approved by the following committee of the Faculty of the Graduate School at the University of North Carolina at Greensboro.

Committee Chair \_\_\_\_\_

Committee Members \_\_\_\_\_

\_\_\_\_\_

\_\_\_\_\_

\_\_\_\_\_  
Date of Acceptance by Committee

\_\_\_\_\_  
Date of Final Oral Examination

## TABLE OF CONTENTS

	Page
LIST OF TABLES .....	vi
LIST OF FIGURES .....	vii
CHAPTER	
I. INTRODUCTION .....	1
I.1 SPRi in the Detection of Clinical Biomarkers .....	2
I.2. Principle of Operation of SPRi Sensors .....	2
I.3. SPRi Sensor Surface Optimization .....	4
I.4 Direct versus Sandwich-Amplification Detection .....	5
II. REVIEW OF THE LITERATURE .....	9
II.1. Sensor Surface Development in SPRi Platforms .....	9
II.1.1 Surface Chemistries and Immobilization Methods .....	9
II.1.2 Peptide and Antibody-Based SPRi Arrays .....	13
II.1.3 Nucleic Acid-Based SPRi Arrays .....	16
II.2. Multitarget Detection Using SPRi Microarrays .....	17
II.3. Signal Amplification Strategies in SPRi Assays .....	19
III. COMPARATIVE ANALYSIS OF HUMAN GROWTH HORMONE IN SERUM USING SPRi, NANO-SPRI AND ELISA ASSAYS .....	21
III. 1 Introduction .....	21
III.2 Methods .....	23
III.2.1 Prepare SPRi Chip for Antibody Array .....	23
III.2.2 Immobilization of Antibody on Functionalized Chip .....	24
III.2.3 SPRi Experiment Setup and Blocking .....	25
III.2.4 SPRi Detection of Human Growth Hormone .....	26
III.2.5 SPRi Data Analysis .....	27
III.2.6 ELISA Protocol .....	27
III.3 Results .....	29

III.3.1 Schematic Representation of Direct and Amplified SPRi .....	29
III.3.2 ELISA Setup and Analysis of RhGH in 10% Serum .....	30
III.3.3 Direct Detection of RhGH in 10% Serum with SPRi .....	32
III.3.4 Amplified Detection of RhGH in 10% Serum with NanoSPRi.....	33
III.3.5 Comparative Analysis of SPRi and NanoSPRi.....	35
III.3.6 Specificity Analysis of NanoSPRi Platform.....	36
III.3.7 Correlation Analysis Between ELISA and SPRi Results .....	37
III.3.8 Kinetic Analysis of the Binding Event in ELISA and SPRi.....	38
III.4 Conclusions .....	39

IV. MULTIPLEX DETECTION OF ORGAN INJURY BIOMARKERS USING SPRI BASED NANO-IMMUNOSENSOR .....	44
---	----

IV.1 Introduction .....	44
IV.2 Methods.....	47
IV.2.1 Materials and Chemicals.....	47
IV.2.2. Sensor Surface Preparation.....	47
IV.2.3. SPRi Measurements.....	48
IV.3 Results.....	50
IV.3.1 Biosensor Surface Optimization.....	50
IV.3.2 Minimizing Non-Specific Interaction.....	51
IV.3.3 Singleplex Measurements of KIM-1 and HMGB-1 .....	53
IV.3.3 Multiplex Measurements of Both KIM-1 and HMGB-1 .....	56
IV.4 Conclusions .....	60

V. ULTRASENSITIVE DETECTION OF PROGESTERONE USING A NANO-SPRI BASED APTASENSOR .....	64
--	----

V.1 Introduction .....	64
V.2 Methods .....	67
V.2.1 Chemicals and Materials.....	67

V.2.2 X-aptamer Selection.....	67
V.2.3 Sensor Chip Functionalization.....	69
V.2.4 Ligand Immobilization.....	69
V.2.5 NanoEnhanced Binding Assay.....	70
V.3 Results .....	71
V.3.1 Screening of Developed X-aptamers .....	71
V.3.2 Direct Detection Assay Measurements .....	73
V.3.3 Specificity Assay Measurements .....	74
V.3.4 Sandwich-Amplification Assay .....	76
V.4 Conclusions .....	78
VI. CONCLUSION AND FUTURE PERSPECTIVES .....	82
REFERENCES .....	84

## LIST OF TABLES

	Page
Table 3.1. Concentrations of The Standards and Controls Included in The Commercial ELISA Kit. ....	28
Table 3.2. Concentrations of the rhGH Samples Prepared in 10% Serum.....	28
Table 3.3. Full Kinetic Data Analysis Including The Evaluation of The Affinity, On-rate and Off-rate of The Antibody Responses Using Graphpad (ELISA) and Data Analysis (SPRi and Nano-SPRi) Software. ....	39

## LIST OF FIGURES

	Page
Figure 1.1. The SPRi Biosensor Setup Based on the Kretschmann Geometry.....	4
Figure 2.1. A Demonstration of Two Strategies for Antibody Immobilization. ....	12
Figure 2.2. A Scheme Representation of the Immobilization of IgG Antibodies to a Protein G (cysteine-Tagged) Coated Surface .....	13
Figure 2.3. (A) The Different SPRi Sensorgrams Representing the Response (angle shift) Obtained with the Different Concentrations of SEA to an Anti-SEA Functionalized Surface.....	15
Figure 2.4. A Scheme Representing the Surface Setup of the Gold Sensor and the Binding Events of CRP Occurring on the Surface. ....	16
Figure 2.5. A Schematic Representation of the Immobilized Mycotoxins and the Selective Detection Using Monoclonal Detection Antibodies Followed by the Signal Enhancement Due to the Introduction of Gold Nanoparticles .....	19
Figure 3.1. A Schematic Representation Comparing Direct-Mode (SPRi) and Amplified-Mode. ....	30
Figure 3.2. A Schematic Representation of the ELISA Assay Procedure. ....	31
Figure 3.3. ELISA Data Analysis .....	32
Figure 3.4. Direct SPRi Detection of rhGH Spiked in 10 % Human Serum .....	33
Figure 3.5. Detection of rhGH Using a Sandwich Assay Spiked in 10 % Human Serum.. ....	34
Figure 3.6. Nano-SPRi Detection of hGH Spiked in Human Serum.....	35
Figure 3.7. A Comparative Analysis of SPRi with Nano-SPRi.....	36
Figure 3.8. Assessment of Nano-SPRi Selectivity to rhGH. ....	37

Figure 3.9. Pearson Correlation Analysis Between ELISA and Nano-SPRi.....	38
Figure 4.1. Comparative Biosensor Behavior in Response to HMGB-1 (4 µg/ml) in Buffer.....	51
Figure 4.2. Comparative SPRi Sensorgrams to HMGB-1 Binding to Two Surfaces Under Different Blocking Conditions.....	53
Figure 4.3. A Concentration Profile of Nanoenhanced SPRi Signal in Response to HMGB-1 in Buffer.....	55
Figure 4.4. A Concentration Profile of Nanoenhanced SPRi Signal in Response to KIM-1 in Buffer.....	56
Figure 4.5. The Step-Wise Experimental Approach in the Design of Sandwich Assay.....	58
Figure 4.6. Multiplex SPRi Sensorgram of KIM-1, HMGB-1 and IL-6 Control.....	60
Figure 5.1. Screening of All X-Aptamers Using SPRi-Based Direct Sensing.....	73
Figure 5.2. A Direct Detection Concentration Profile of SPRi Response of Progesterone in Buffer.....	74
Figure 5.3. A Specificity Assay Comparing the SPRi Response of Positive X-Aptamer 5 to Progesterone and β-estradiol.....	76
Figure 5.4. A Sandwich-Amplification Assay Concentration Profile of Progesterone in Buffer.....	78

## CHAPTER I

### INTRODUCTION

Biological markers also known as biomarkers are present in all body parts and tissues. The detection of biomarkers in bodily fluids has been the goal of clinical diagnostic techniques mainly in order to obtain a better understanding of the physiological processes related to disease progression as well as the evaluation of the efficacy of therapeutic treatments. This has led to the development and continuous improvement of proteomic technologies that can identify novel biomarkers in a reliable and sensitive manner. Gel electrophoresis [2], mass spectrometry [3], matrix-assisted laser desorption/ionization mass spectrometry (MALDI-MS) [4], real time polymerase chain reaction (PCR) quantification of protein biomarkers [5], and antibody-array assays such as the common enzyme linked immunosorbent assay (ELISA) [5] have become widely used direct analysis tools that assess biomarker activity and concentration in body fluids. These technologies have served in the validation of biomarker activity and have provided quantitative data for specific target proteins; however, better alternatives have emerged to meet the challenges of developing better quality and more reproducible assays.

Optical singleplex and multiplex detection of critical biomarkers in serum or blood is one example, which has been shown to provide excellent sensitivity and reproducibility [6]. The specificity and sensitivity of this detection method has proven to

be suitable for clinical use, as accurate measurements have been achieved. Surface plasmon resonance imaging lies at the forefront of optical tools that can detect and study biomarkers in a label-free and real-time manner.

### **I.1 SPRi in the Detection of Clinical Biomarkers**

Surface plasmon resonance imaging (SPRi) is one the most popular optical technologies used to study biomolecular interaction at the nanoscale level on a metal-coated surface. This tool is characterized by its label-free and real-time nature in the quantitative analysis of biomolecular processes. The inherent properties offer a major advantage over other widely used techniques, as it is capable of enhancing the sensitivity and specificity of the detection process. The sensing capabilities of this technology have been extended to analyze a range of biomolecular recognition events and binding types. Protein- protein [7-10], protein-DNA [11, 12], protein-antibody [13, 14], protein-cell [15], antibody-cell [16, 17], toxin-receptor [18] have been at the focus of the many applications of this platform.

### **I.2. Principle of Operation of SPRi Sensors**

SPRi biosensors require the immobilization of a ligand (antibody, protein, DNA, toxin, bioreceptor.... etc.) onto a thin metal-coated surface (mostly gold) as it is a good starting point for further surface modifications. This optical technique utilizes the changes in refractive index at the interface between the metal surface and the medium of interaction as means for the detection of the analyte in solution (Figure 1.1 A&B). The sensing mechanism utilizes an incident monochromatic light that hits the sensor surface, a detector that collects the resulting reflected light and a CCD camera that generates a

real-time contrast image. The sensor surface consists of a high index prism, coated with a chromium adhesion layer (5 nm) and a gold layer (50 nm) where the ligands of interest are immobilized. At a specific incident angle known as the resonance angle, the impinging light excites the free electrons in the gold layer; resulting in an evanescent field (up to ~400 nm thick); which exponentially decays from the sensor surface. And this in turn leads to a minimum intensity in the reflected light. The surface plasmons thus created are sensitive to perturbations in the refractive index of the surrounding medium; and a detector measures these alterations as changes in the reflectivity signal. The SPRi apparatus also allows a real-time visualization of the sensing surface for multi-array purposes by intercepting the reflected light with a CCD camera to provide a contrast image representing the biomolecular interactions at the surface [19].

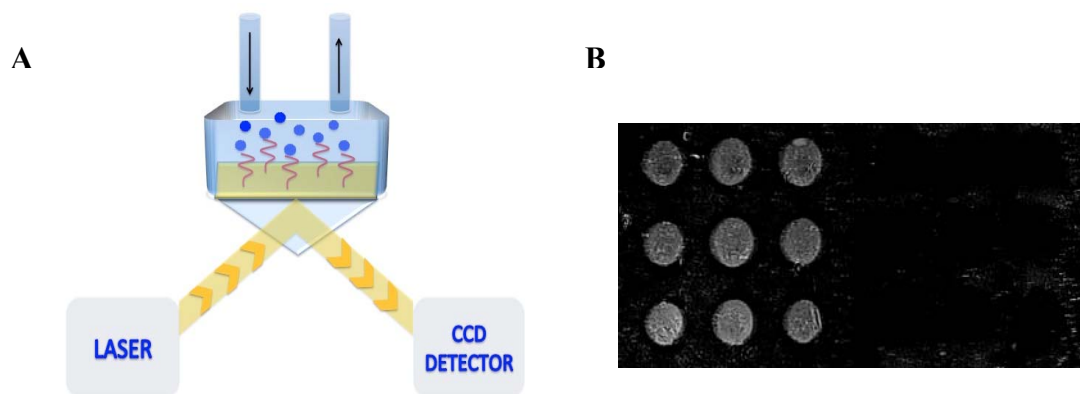


**Figure 1.1. The SPRi Biosensor Setup Based on the Kretschmann Geometry. (A) The light incident on the metal surface excites the surface plasmons causing a dip in the reflected light. (B) A CCD detector collects the reflected light and generates a digital difference image reflecting the binding events on the sensor surface. Bright spots represent regions of specific-biomolecular interaction and dark regions represent the absence of biomolecular interaction.**

### **I.3. SPRi Sensor Surface Optimization**

At the heart of SPRi biosensors lies the sensor surface design as the primary building block in assay development. In fact, the sensor surface has a tremendous role in determining the performance of the biosensor in different applications. Hence, it is crucial to develop optimal surface chemistries that can mimic biological environments while maintaining the functionality of immobilized ligands. The metal-coated sensor surface serves as the substrate that is treated with various chemistries to enable the linking of ligands to the biosensor surface. There are two major aspects to take into account when a surface is treated for analyzing biomolecular interactions. First, a proper surface architecture is important for a qualitatively and quantitatively efficient

immobilization of capture ligands. In this process, steric hindrance, amount of ligand immobilized, biological activity, and orientation of ligand are all influenced by the selected nanostructured sensor surface. The second factor in the design of label-free assays is the homogeneous bioinertness of the sensor surface that minimizes the non-specific adsorption of protein and other macromolecules present in complex bodily fluids. This process is known as surface blocking; hence, the ratio of specific signal to non-specific signal will be high.

#### **I.4 Direct versus Sandwich-Amplification Detection**

The detection of biomolecular events using SPRi can be carried out by two main strategies, direct or indirect. The direct mode of detection as the name implies, involves the detection of biomolecules in solution upon the interaction with the immobilized ligands in the solid phase. This is performed without the need for secondary markers or labels. On the other hand, indirect detection (sandwich amplification assay) involves the introduction of signal enhancing probes that bind to the analyte bound to the immobilized ligands in order to improve the sensitivity of the assay. Therefore, signal amplification probes have extended the application of SPRi to include small analyte resulting in ultrasensitive assays.

In the following chapters, we demonstrate the development of ultrasensitive SPRi sensor assays based on specific monoclonal capture antibodies and x-aptamers for the detection of different biological molecules. In these studies, we incorporated the label-free, real-time, and multiplexing capabilities of SPRi with signal amplification probes (near-infrared quantum dots) for achieving ultrasensitive limits of detection of

biomolecules in serum and buffer. Moreover, we introduced significant improvement in sensor surface design, which is a critical step in the development of a reliable assay.

In our first work, we developed a SPRi immunoassay and introduced signal amplification probes for the detection of the recombinant human growth hormone (rhGH) in serum. The ultrasensitive detection of hGH is essential as it is linked to numerous growth disorders and used by athletes as a doping agent for enhanced physical performance. The hGH immunosensor was developed by the covalent attachment of monoclonal hGH antibodies to the sensor surface and by further blocking the surface using bovine albumin serum (BSA). Blocking the sensor surface was performed to minimize the non-specific adsorption of proteins and biomolecules present in serum. Upon successful optimization of sensor design, direct detection of hGH at different concentrations in serum was performed and the limit of detection was determined to be 3.6 ng/mL. Further addition of signal amplification probes, pre-functionalized with hGH secondary antibodies, allowed a detectable signal to be achieved at lower concentrations with a limit of detection of 9.1 pg/mL. The results of these two assays were compared to an hGH ELISA assay performed at different concentrations in serum which resulted in a LOD of 1 ng/mL. As can be deduced, the conventional analysis tool (ELISA) was similar in sensitivity to the direct SPRi measurements. However, the enhancement in sensitivity was accomplished with the incorporation of amplification probes to the immunoassay (Nano-SPRi). The ultrasensitive capability in addition to reproducibility and short detection time impart the robustness and novelty to the Nano-SPRi assay over conventional ELISA assays. The results achieved with this immunosensor have led to a

multiplex study, which assessed the multi-target detection of disease related biomarkers, KIM-1 and HMGB-1 in buffer.

In the second study, we employed a specific antibody-based SPRi assay in combination with signal enhancers for the ultrasensitive measurement of HMGB-1 and KIM-1 in a singleplex and multiplex manner. The immunosensor surface was designed differently from the one previously reported for the purpose of enhancing the sensitivity and reproducibility of the platform. We adopted a non-covalent attachment approach for monoclonal KIM-1 and HMGB-1 capture antibodies to the sensor surface. We chose to pursue with the non-covalent attachment of antibodies because this results in well-oriented ligands in comparison with the amine coupling of antibodies, which leads to random immobilization on the sensor surface. The surface was further blocked using a combination of BSA and polyethylene glycol (PEG) to decrease the non-specific adsorption of proteins. As a result, a robust immunoassay was obtained and used in combination with signal enhancers for the singleplex and multiplex analytical measurement of HMGB-1 and KIM-1 with a limit of detection of 5 pg/mL in buffer.

Our next approach aimed at performing small molecule sensing using a nanoenhanced SPRi aptasensor. Progesterone, a steroid hormone responsible for multiple reproductive processes in the female body was the target analyte in this assay. Its detection can assist in the early diagnosis of pregnancy as well in fertility investigations. For the purpose of the ultrasensitive detection of progesterone, specific x-aptamers were developed as the capture ligands and nanoenhancers were introduced again to assay procedure. The capture ligands were immobilized on the sensor surface and progesterone

levels was directly measured in buffer as well as indirectly to achieve a LOD of 1 nM. As a result, this work introduced a novel, reliable, and sensitive aptasensor that detected progesterone at ultra-low concentrations.

## CHAPTER II

### REVIEW OF THE LITERATURE

#### **II.1. Sensor Surface Development in SPRi Platforms**

The performance of a biosensor is highly influenced by the surface development, which represents the primary building block in the assay design. In this step, it is critical to design a reproducible platform while retaining the activity of biological molecules. This process begins with a bare gold surface, which manifests a high affinity for soft electron pair donors such as thiolated compounds. Hence, the thiol-gold bonding character is a widely employed surface treatment method in self-assembly because the thiolated compounds adsorb spontaneously on the metal surface and serve as a strong support for the anchored ligand of interest.

##### *II.1.1 Surface Chemistries and Immobilization Methods*

Sensor surface development can be accomplished by two methods, either by utilizing thiolated linkers (alkanethiols) [20-22] to immobilize the ligand or a thiol-modified ligand directly attached to the sensor surface [23, 24]. For example, Mannelli *et al.* developed an efficient sensor to monitor the hybridization of DNA anchored on the metal surface [25] by functionalizing the bare gold surface with 11-mercaptoundecanoic acid-poly (ethylenimine) and exposing the amine-reactive surface to an extravidin solution, which is further allowed to support the biotinylated DNA [26, 27] by the strong

affinity avidin-biotin interaction. Similarly, amine terminated alkanethiols were reacted with a bare gold surface by the thiol ends and to chicken ovalbumin and immunoglobulin G by the amine terminated ends. These biomolecules were used as models for different glycoproteins that could potentially be identified and analyzed using SPRi [28]. In addition, thiol modified ligands can be directly attached to the sensor surface without the need of linkers, and Manera *et al.* have immobilized thiolated DNA onto lithographically-patterned gold surface to monitor the hybridization of the 35S promoter oligonucleotide probe [27] as a way to detect for genetically modified organisms inserted into a host genome. Similarly, Song *et al.* were able to detect two specific genes of *Arabidopsis thaliana* leaf extract at attomole concentrations using thiol-modified DNA probes [29].

Another approach utilizing ligand attachment in antibody immobilization [30, 31] involves the activation of carboxyl groups of alkanethiols directly adsorbed onto the surface by 1-ethyl-3-(3-dimethylaminopropyl) carbodiimide hydrochloride (EDC)/ N-Hydroxysuccinimide (NHS). This activation step yields an amine-reactive surface via reactive esters [32] and forms a supporting layer for amine-containing compounds. For example, an immunosensor was developed for early cancer diagnosis by selectively identifying potential cancer biomarkers using an anti-activated leukocyte cell adhesion molecule/CD 166 (ALCAM) and anti-transgelin-2 (TAGLN2) immobilized on an EDC/NHS activated surface [33].

A variety of surface chemistries have been developed for SPRi-based applications. Advances have also emerged to improve the performance of biosensors; for instance, amine coupling of specific antibodies with amine-reactive surface is not optimal

for reliable and reproducible results in immunosensors. This is mainly due to the random attachment of ligands onto the surface resulting in an uncontrolled orientation of the ligand, and a reduction in the biological activity of the biomolecule (Figure 2.1). With these limitations in mind, alternative strategies were needed and one study was able to take advantage of binding properties of protein G produced by genetically engineered *Streptococcus* bacteria which introduces cysteine residues at specific sites of the protein [34]. Cysteine residues, which contain thiol groups, can adsorb on the gold surface and form a layer of protein on the sensor surface. Protein G has a specific binding site for the fragment crystallizable (Fc) region of antibodies; hence, participating as an affinity receptor for antibody immobilization (Figure 2.2). This approach results in well-oriented antibodies and reproducible sensing platforms with enhanced sensitivity [35].

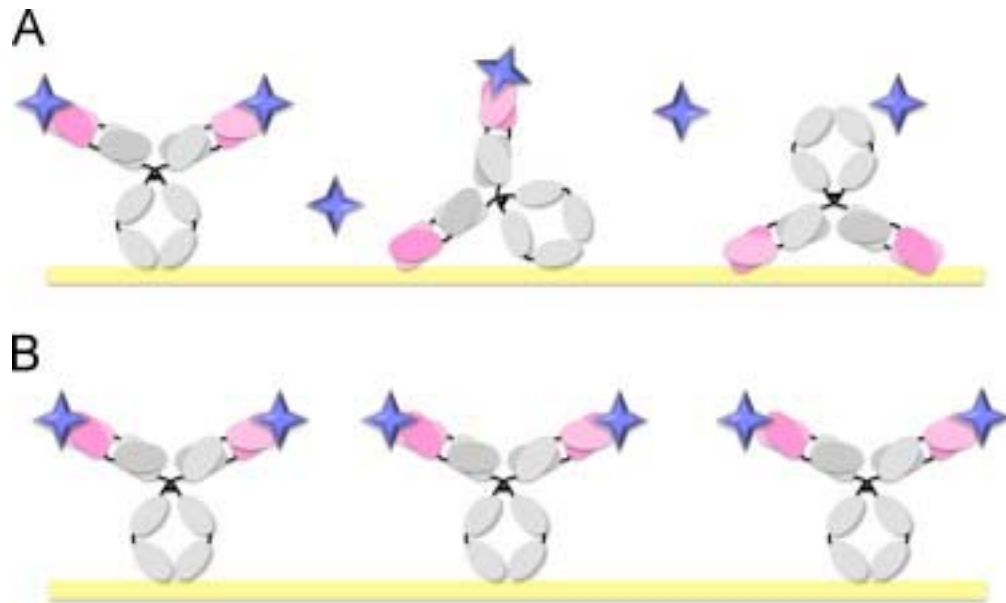


**Figure 2.1. A Demonstration of Two Strategies for Antibody Immobilization. (A) Random antibody immobilization (A) and site-directed antibody immobilization (B) [1].**

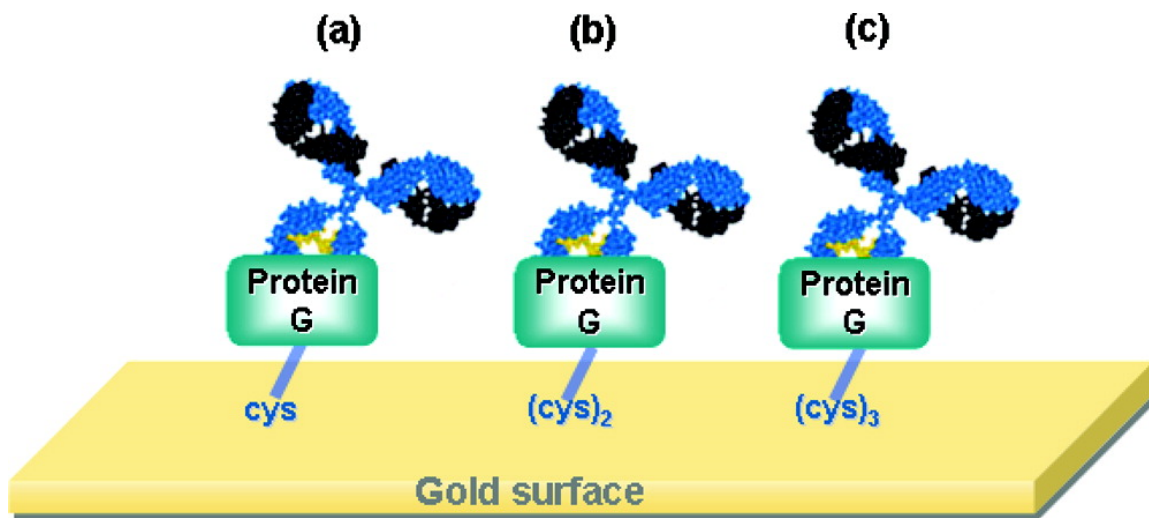


**Figure 2.2. A Scheme Representation of the Immobilization of IgG Antibodies to a Protein G (cysteine-tagged) Coated Surface <sup>1</sup>.**

### *II.1.2 Peptide and Antibody-Based SPRi Arrays*

The study of antibody-antigen interaction can be achieved using SPRi-based microarrays and has been reported in numerous studies. In one study, chicken polyclonal antibodies specific for *M. Synoviae* were assessed in a rapid, label-free and peptide-chip SPRi platform. The sensor surface was immobilized with lipoprotein major surface protein (MSPB) and hemagglutinin MSPA as the specific antigens responsible for the serodiagnostic measurement of anti-MSPA levels in chicken serum [36]. Ro *et al.* constructed another peptide-based assay for the analysis of protein-protein interaction for a better understanding of these basic cellular regulatory processes. Human papillomavirus (HPV) was chosen as the model study and the interaction of surface attached-HPV E6AP

<sup>1</sup> Reprinted “Lee, J.M., et al., Direct immobilization of protein g variants with various numbers of cysteine residues on a gold surface. *Anal Chem*, 2007. 79(7): p. 2680-7”. Copyright (2007) with permission from American Chemical Society.

with P53 and E6 was assessed resulting in a detectable and quantitative SPRi response that reflects the binding events between these proteins [37].

In response to the need for reliable methods that can detect food borne pathogens, and in specific staphylococcal enterotoxin A (SEA), a SPRi immunosensor was functionalized using a self-assembled monolayer (SAM) onto which anti-SEA were directly immobilized. This platform exhibited a specific and sensitive detection of the toxin in buffer and in both phosphate buffer and milk at a concentration range of 100-1000 ng/mL as shown in Figure 2.3 [38].

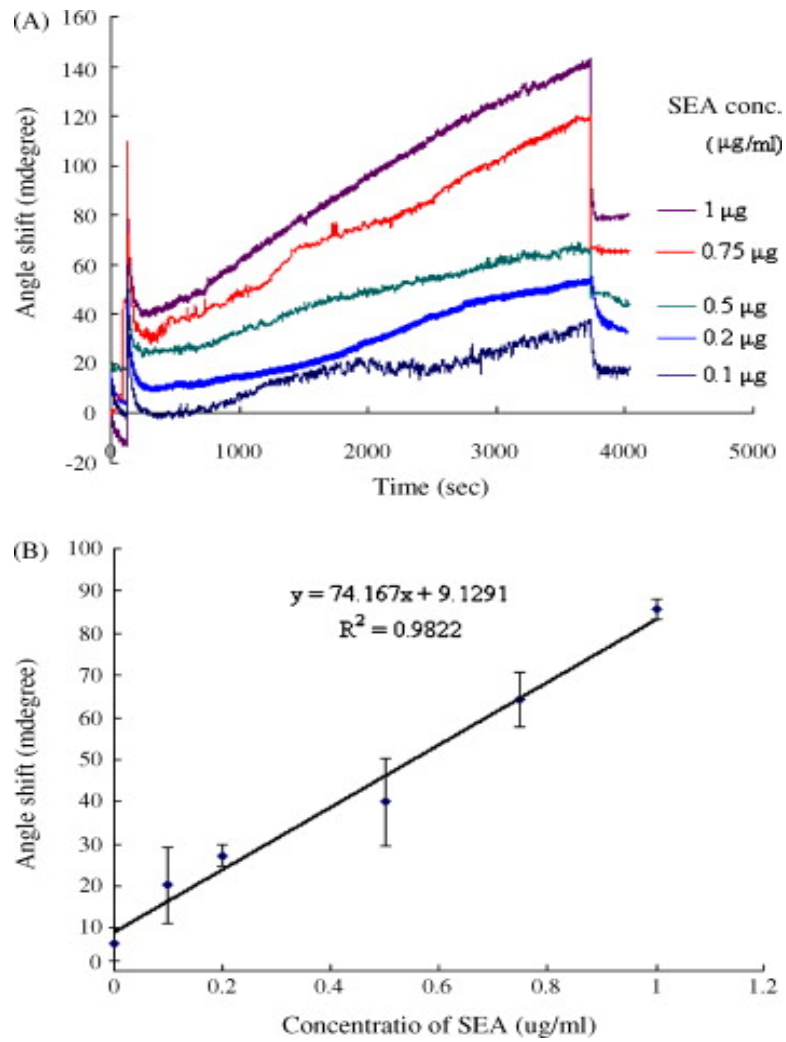


**Figure 2.3. (A) The Different SPRi Sensorgrams Representing the Response (angle shift) Obtained with the Different Concentrations of SEA to an Anti-SEA Functionalized Surface. (B) A Concentration Standard Curve of the SPRi Response (angle shift) versus the Concentrations of SEA Interacting with Anti-SEA Functionalized Surface in Phosphate Buffer <sup>2</sup>.**

In addition, human inflammation markers in the blood serum such as the C-Reactive Protein (CRP) represent a classical target in many SPRi studies due to the

<sup>2</sup> Reprinted from Sensors and Actuators B: Chemical SPR-based immunosensor for determining staphylococcal enterotoxin A, 136, Tsai, Wen-Chi, Li, Ie-Chin, 8-12. Copyright (2009), with permission from Elsevier.

enhanced sensitivity and selectivity of this detection technique [39-42]. Meyer *et al.* investigated the potential of an anti-CRP immunosensor for the direct measurement of CRP levels in buffer while taking advantage of the kinetic analysis to determine the association and dissociation rates of CRP from two different antibodies [43]. The detection of CRP was performed by the assistance of a detection antibody (C2) that binds the already surface bound CRP (Figure 2.4).

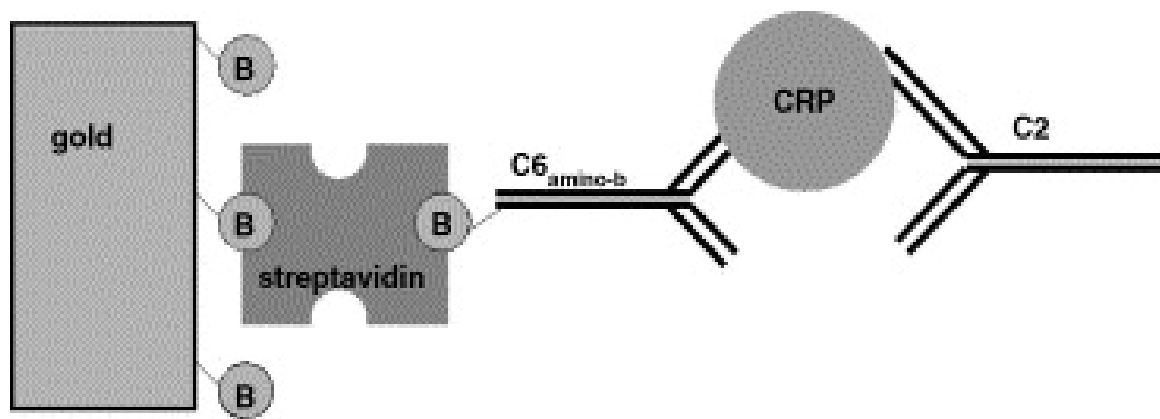


**Figure 2.4. A Scheme Representing the Surface Setup of the Gold Sensor and the Binding Events of CRP Occurring on the Surface. A biotin-streptavidin binding allows the attachment of the selective anti-CRP to the surface. A detection antibody (C2) is injected following the addition of CRP forming the reported detection signal**

<sup>3</sup>.

### II.1.3 Nucleic Acid-Based SPRi Arrays

SPRi has gained increased interest as a promising analysis tool for the detection, quantification, and understanding of nanoscale biomolecular events occurring on the

---

<sup>3</sup> Reprinted from Biosensors and Bioelectronics, SPR-based immunosensor for the CRP detection—A new method to detect a well known protein, 21, Martin H.F. Meyer, Markus Hartmann, Michael Keusgen, 1987-1990., Copyright (2006), with permission from Elsevier.

metal surface of a biosensor. This has led to numerous studies in the area of DNA identification and interactions with complementary biomolecules. For example, Corn's research group successfully developed innovative surface treatments to optimally attach a variety of oligonucleotides (DNA and RNA) to the metal surface for analysis. Assessing the binding and catalytic properties of the repair enzyme DNA N-glycosylase and the binding of repair proteins to damaged regions of DNA was accomplished by an array of oligonucleotides [44]. Single-stranded oligonucleotide microarrays were also employed to detect the of Roundup Ready soybean lectin gene sequences by real-time monitoring of the hybridization of the target PCR products and DNA or PCR-generated probes [45]. DNA based microarrays have proven capable of differentiating between close nucleotide sequences which has extended their application to assessing gene mutations for gaining a better understanding of cystic fibrosis [46].

## **II.2. Multitarget Detection Using SPRi Microarrays**

SPRi assays are characterized by their microarray ability, which entails a highly versatile analysis tool for the simultaneous detection of multiple interactions on the sensor surface in a high-throughput manner. This sensing capability successfully meets the future needs of medical diagnostics and is made possible by the imaging component, which allows the selection and identification of numerous spotted ligands on the surface for analysis. Piliarik *et al.* developed a multiplex platform for the screening of protein biomarkers involved in cancer diagnosis and were able to achieve significantly sensitive limits of detection as low as ng/mL concentrations in blood plasma [40]. The platform developed for this purpose uniquely combined specific antibodies and DNA spotted on

the surface. The surface was primarily functionalized with thiolated oligonucleotide sequences and the specific antibodies were immobilized in a well-directed manner by conjugation to an oligonucleotide sequence that is complementary to the spotted oligonucleotide sequence, which can directly hybridize to the sensing area. Furthermore, The multiplex monitoring of three allergens in milk was performed using a biosensor immobilized by the 3 allergens,  $\alpha$ -lactalbumin,  $\beta$ -lactoglobulin and casein and specific antibodies for each flowing above the surface. This analysis assisted in obtaining the avidity of the interaction by monitoring the kinetics of the association and dissociation of the antibody-allergen in real-time [47]. The performance of SPRi multi-target arrays was also tested for the immunodetection of antimicrobial drugs in milk residue in order to provide a better assessment of consumer health risks [48].

The implications of this sensing capability have also extended to detect small molecules, which can be very challenging in SPRi based platforms. Mycotoxins are one example and their interaction with complementary antibodies was assessed in one study [49] to achieve detectable signals at low concentrations. The low limit of detection (pg/mL levels) was obtained due to the use of gold nanoparticles as signal enhancement probes that were added as the last step of the assay shown in Figure 2.5.

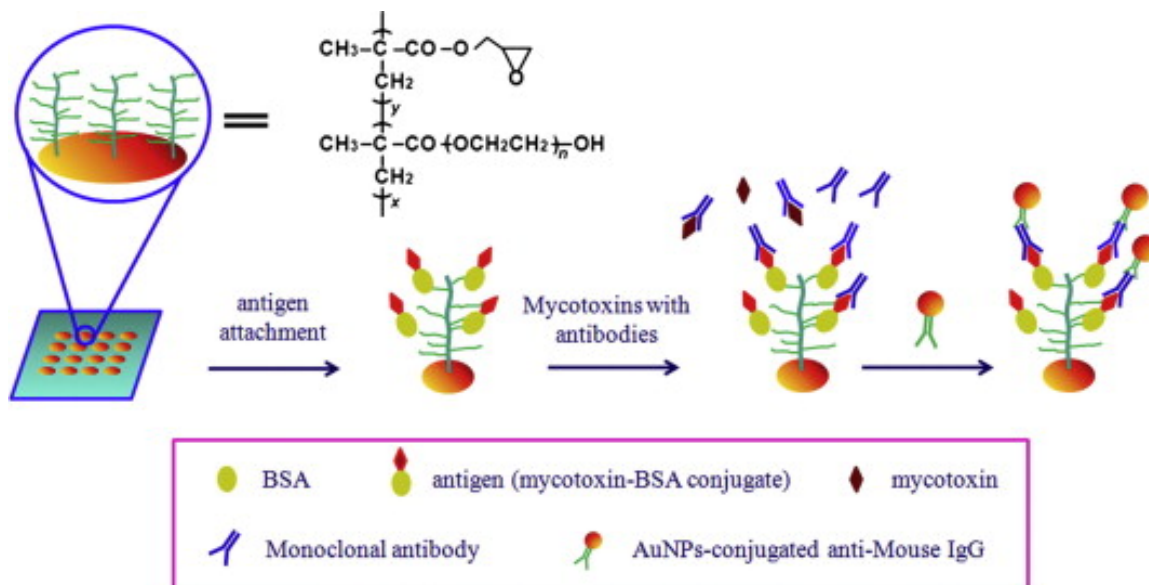


**Figure 2.5. A Schematic Representation of the Immobilized Mycotoxins and the Selective Detection Using Monoclonal Detection Antibodies Followed by the Signal Enhancement Due to the Introduction of Gold Nanoparticles**<sup>4</sup>.

### II.3. Signal Amplification Strategies in SPRi Assays

Currently, SPRi is used for industrial as well as academic research in screening biomolecular activity due to its label-free and real-time analysis; however, this tool still faces some limitations and there is room for improvement. This is mainly manifested in small molecule sensing imposed by the mass loading effect as the major factor causing the change in reflectance reported as the SPRi response. As a result, researchers have dedicated time and effort to investigating the optimization of the platform and employing signal enhancers [50] that would indirectly amplify the SPRi response as a method to increase the sensitivity of the platform. Numerous approaches have been reported that

<sup>4</sup> Reprinted from the Journal of Colloid and Interface Science, Sensitive detection of multiple mycotoxins by SPRi with gold nanoparticles as signal amplification tags, 431, Hu, W., et al., 71-76., Copyright (2014), with permission from Elsevier.

utilize metal nanoparticles as indirect labels. Examples include gold nanoparticles [51, 52], magnetic nanoparticles [53], and quantum dots [54, 55].

Malic *et al.* were one of the first to apply quantum dots as amplification labels to enhance the diagnosis potential of SPRi-based platforms. The platform was designed for the detection of single stranded DNA (ssDNA) and a cancer biomarker, prostate-specific antigen conjugated to antichymotrypsin (PSA-ACT). In both immunoassays, the addition of the near infrared quantum dot complexes resulted in significant enhancement; 25 fold enhancement for ssDNA with a limit of detection (LOD = 100 fM) and 50 fold for PSA-ACT (LOD = 100 pg/mL). An important finding of this work was the noticeable difference between the amplification effect of 800 nm QDs whose emission wavelength is the same as the emission wavelength of the light source used to excite the surface plasmons of the gold layer the remaining different sized QDs. The resonant coupling between the emitting 800 nm QDs and the propagating surface plasmons as well as the large mass of these nanoparticles were two reasons responsible for the signal amplification effect [55].

CHAPTER III  
COMPARATIVE ANALYSIS OF HUMAN GROWTH HORMONE IN SERUM  
USING SPRI, NANO-SPRI AND ELISA ASSAYS

**III. 1 Introduction**

Human growth hormone (hGH) is a 191 amino acid peptide (22 kDa) produced by the pituitary gland and directly released into the bloodstream. Interactions between the hypothalamic peptide growth hormone-releasing hormone (GHRH) and somatotropin induce pulsatile secretions of hGH. As a result, levels of hGH vary from highs in the 50-100 ng/mL to lows in the 0.03 ng/mL range [56]. Deficiency or excess of hGH in the body can provoke a wide range of abnormal physiological symptoms. For example, excess levels of hGH can lead to gigantism [57] and diabetes [58]. Depleted levels of hGH cause low blood sugar in newborns, and weak bone density and depression in adults [59].

The administration of the recombinant form of hGH (rhGH) improves lean muscle mass while reducing body fat. As such, this substance became the drug of choice for professional and amateur athletes as it improves physical strength that confers an advantage in competitive sports. rhGH is banned by the World Anti-Doping Agency (WADA) [60, 61] and much effort by international researchers has been focused on developing tests that can detect its presence or anabolic effect. Enzyme-linked immunosorbent assay (ELISA) has been the preferred method for the determination of

hGH in whole blood [62]. Although, ELISA is a reliable technique offering good sensitivity and selectivity, it is relatively time- and labor-intensive. In addition, ELISA relies on the indirect detection of hGH by employing enzymatic tags. In contrast, surface plasmon resonance (SPR) permits detection of hGH directly without the use of labels in real time. The detection principle behind SPR involves a sensing surface consisting of a prism that is coated with a thin metal layer (gold or silver); when a monochromatic polarized light interacts with the metal surface, “surface plasmons” are generated. The binding of an analyte to a surface receptor immobilized on the metal surface perturbs the resonance conditions resulting in a shifted resonance dip, which can then be correlated to the analyte concentration. SPR-based biosensors are now commercially available that offer a real-time, label free technique to monitor biomolecular binding events and biochemical reactions [63-65]. More recently, SPRi was developed in response to the need for multiplexing (i.e. monitoring multiple binding events simultaneously), which was not possible in classical SPR biosensors. Thus, SPRi has emerged as a tool to monitor several binding events simultaneously. Current SPRi systems are based on microscopic imaging of a surface which is excited with light at a specific angle and wavelength [65]. The image is then captured onto a charge-coupled device (CCD) array.

To date, there have been a few SPR-based assays developed to detect hGH [66-69]. One particular strategy, known as the isoform method [70], relies on the detection of the ratio of 22 kDa hGH to total hGH, as non-22-kDa endogenous levels drop after exogenous rhGH administration. Recently, de Juan-Franco *et al.* [66] reported on the development of a SPR-based immunosensor for the selective detection of the 22 kDa and

20 kDa hGH isoforms in human serum samples. Monoclonal antibodies specific to each isoform were immobilized directly on the gold sensor permitting the measurement of both isoforms simultaneously in a single injection with a limit of detection at  $0.9 \text{ ng mL}^{-1}$ . Alternatively, SPR has been used to screen antibodies with high specificity to hGH [68]. If the concentration of target analyte falls below the SPRi system's limit of detection ( $< \text{nM}$ ), one has to resort to amplifying the SPRi signal via the utilization of nanoparticles (Nano-SPRi). Such SPR-based amplification has been well documented in the literature [55, 71-73] for various types of analyte and surfaces.

In this work, the analytical potential of SPRi and Nano-SPRi based biosensors was examined, particularly for the detection of rhGH in spiked human serum, and comparison of its detection capability directly to ELISA. The following parameters will be reviewed and considered: detection time, sensitivity, kinetic profile, reproducibility and specificity.

## **III.2 Methods**

### *III.2.1 Prepare SPRi Chip for Antibody Array*

A bare gold biochip is cleaned by sonication in a stabilized piranha solution (3:1 concentrated sulfuric acid to 30% hydrogen peroxide) for 90 minutes at  $50 \text{ }^\circ\text{C}$ . This is followed by rinsing, sonication with water for 5 minutes, rinsing with ethanol and finally dried with nitrogen stream. The clean gold chip is then placed in an UV/Ozone chamber (30 mins) to remove any contaminants. The surface functionalization follows by a microwave radiation assisted procedure. The first step involves reacting the surface with an 11-mercaptoundecanoic acid (11-MUA) solution (34 mM, in pure ethanol) under

microwave radiation (50 W and 50 °C) for 5 minutes. A sequential thorough ethanol and water rinse step follows this reaction. The second step reacts the carboxyl groups of 11-MUA with a 1-ethyl-3-(3-dimethylaminopropyl) carbodiimide (EDC) solution (65 mM in ultrapure water) under the same microwave conditions (50 W and 50 °C) for 5 minutes. The chip is then rinsed with ultrapure water to ensure the removal of unreacted chemicals. The third reaction involves another microwave irradiation (50 W, 50 °C, for 5 mins) of a N-hydroxysuccinimide (NHS) solution (40 mM in ultrapure water). And the last step involves blocking the sensor surface with a polyethylene glycol (PEG800) solution (250  $\mu$ M in ultrapure water) under microwave irradiation (50 W, 50 °C, for 5 mins) and then rinsed with an ultrapure solution prior to immobilizing the anti-rhGH antibody. Microwaving PEG800 on the surface of the sensor is performed as a blocking step to prevent non-specific binding of serum proteins and quantum dot complexes later used in the experiment. This is achieved by PEG800 reacting with non-occupied bare gold sites on the chip.

### *III.2.2 Immobilization of Antibody on Functionalized Chip*

A solution of anti-rhGH antibody (15  $\mu$ g/mL) and negative control (15  $\mu$ g/mL) solution of anti-Immunoglobulin G (anti-IgG) are prepared in a 10% glycerol phosphate buffer solution (PBS, 10 mM) solution. Both samples are then loaded to two separate wells in a 384 well plate.

An array pattern is designed using the LabNext microarrayer (4x7 quadrants for each sample) and the ligands are spotted on the chip using a 500  $\mu$ m Teflon tipped pin.

The sensor chip is allowed incubation time of 2 hours at room temperature and under a humid atmosphere of 75% or greater. Finally, prior to carrying out the SPRi experiment, the sensor chip is rinsed and soaked in ultrapure water and dried with nitrogen stream.

### *III.2.3 SPRi Experiment Setup and Blocking*

The SPRi Lab+ instrument is initiated and the sensor chip is loaded to its position in contact with the flow cell inside the apparatus. The sensor chip is rinsed with ultrapure water initially. Following this loading step, a low salt PBS buffer (10 mM phosphate, 150 mM sodium chloride, pH 7.4) is flown above the surface at a rate of 1 mL/min for a total of 5 mL and then the flow rate is slowed down to 20  $\mu$ L/min and allowed to stabilize for 20 minutes. Prior to analysis, a set of experimental conditions is chosen and one of which is the selection of the highly contrasted difference image of the sensor chip. This digital image provides a real time visualization of the surface and allows the operator to select and define the areas of interest on the surface (400  $\mu$ m spots). Another step is to trace the plasmon curves done by the instrument and choosing a working angle at which the highest slope in reflectivity curves is obtained.

The next step introduces the first blocking agent, a bovine serum albumin (BSA) solution (100  $\mu$ g/mL) prepared in the running buffer. BSA is injected to covalently bind to the amine reactive surface, the remaining unbound BSA will wash off the surface through buffer rinse. A solution of sodium acetate (10 mM) is injected and a high salt PBS (10 mM phosphate, 750 mM sodium chloride, pH 7.4) injection follows to wash the surface. The amine reactive surface is further deactivated by ethanolamine (1 mM). Another surface wash by sodium acetate (10 mM) is performed after this step.

Ultimately, preceding the successful blocking and deactivation of the surface, the running buffer is switched to a 10 mM PBS with 50  $\mu\text{g}/\text{mL}$  BSA solution and a flow rate of 250  $\mu\text{L}/\text{min}$  for a total of 5 mL. BSA (50  $\mu\text{g}/\text{mL}$ ) is added to the running buffer for additional blocking of the surface by non-covalently occupying the non-specific sites and this is done to further reduce non-specific binding of serum proteins to the surface. Finally, the running buffer flow rate is slowed down to 5  $\mu\text{L}/\text{min}$  for the kinetic monitoring.

#### *III.2.4 SPRi Detection of Human Growth Hormone*

Initially, a solution of a set concentration of rhGH (30,000  $\text{pg}/\text{mL}$ ; 250  $\text{pg}/\text{mL}$ ; 25  $\text{pg}/\text{mL}$ ; 2.5  $\text{pg}/\text{mL}$  and 0.25  $\text{pg}/\text{mL}$ ) in 10% serum is prepared and diluted in PBS containing 1  $\text{mg}/\text{mL}$  BSA. And a 2:1 solution of biotin labeled anti-rhGH detection antibodies (6  $\mu\text{M}$ ) and streptavidin coated near infrared quantum dots (1  $\mu\text{M}$ ) is prepared and incubated for 30 min for effective coupling. Then the rhGH prepared sample is injected into the flow cell and the SPRi HORIBA software records the kinetic monitoring of the interaction. Since this interaction results in some non-specific interaction of the serum proteins, the surface is washed with a sodium chloride (450 mM in running buffer) solution prior to the signal amplification step. The previously prepared solution of anti-rhGH detection antibodies and quantum dots is diluted to a concentration of 10 nM (2:1) with running buffer (PBS with 50  $\mu\text{g}/\text{mL}$  BSA) and injected into the flow cell. Following the injection of the rhGH spiked human serum and quantum dot enhancer, an increase in reflectance change occurs due to the amplified shift of the plasmon curves. This results in a difference image showing a gray scale image correlating to the signal of on the chip.

### *III.2.5 SPRi Data Analysis*

The kinetic data is imported into a data analysis program and the SPRi signal (% $\Delta$  Reflectivity) is plotted versus time (s) to determine the difference between the anti-rhGH and negative control antibody spots after the high salt wash.

### *III.2.6 ELISA Protocol*

The ELISA assay was performed using a commercially purchased kit (Invitrogen) and the manufacture protocol was followed for assay preparation and analysis. All assay components included in the rhGH ELISA kit are stored at 2-8 °C when not in use. This includes the anti-rhGH antibody coated well plates, standards (0-5) in sheep serum, controls (1 &2) in human serum, conjugate buffer, (200X) wash buffer, chromogen TMB (Tetramethylbenzidine) and stop reagent. Prior to assay setup, the anti-rhGH antibody coated 96-wells is warmed to room temperature and the desired number of 8-well strips for assay is removed while keeping the remaining wells sealed in the foil package to store at 2-8 °C. The standards are prepared by reconstitution in 2 mL distilled water for standard #0, in 1 mL of distilled water for standards (1-5), and in 1 mL of distilled water for the controls (1&2). Below is a table of the corresponding concentrations of the standards and controls (Table 3.1).

**Table 3.1. Concentrations of The Standards and Controls Included in the Commercial ELISA Kit**

<b>Standards</b>	<b>Concentration (ng/mL)</b>
0	0
1	0.17
2	0.94
3	2.63
4	10.4
5	26.9
Control #1	1.22 ± 0.33
Control #2	4.97 ± 1.25

The samples, which consist of the rhGH hormone in 10% human serum, are prepared at the following concentrations (Table 3.2).

**Table 3.2. Concentrations of the rhGH Samples Prepared in 10% Serum.**

<b>Sample</b>	<b>Concentration (ng/mL)</b>
1	0.025
2	0.2
3	0.5
4	2.5
5	10
6	30

The standards, controls and samples (50 µL) are added to each well (in triplicates) and the wells are sealed and incubated overnight at 4 °C under gentle shaking. The plate is removed from the shaker the following day and allowed to warm to room temperature (15-20 mins) prior to proceeding with the assay. And the Anti-rhGH-HRP, conjugate

buffer, wash buffer (200x), chromogen TMB (tetramethylbenzidine), and stop reagent are all removed from the refrigerator and allowed to warm to room temperature as well. The anti-rhGH-HRP is diluted 40x with the conjugate buffer and the wash buffer is diluted 200x with distilled water. Anti-rhGH-HRP conjugate (50  $\mu\text{L}$ ) is added into each well, and the wells are sealed and incubated at room temperature for 30 minutes while gently shaking. The solution is then decanted from the wells by inverting the plate, tapping it dry onto an absorbent tissue, and then washed with wash buffer (200  $\mu\text{L}$ ) into each well for three times. A solution of chromogen (100  $\mu\text{L}$ ) is then added into each well within 15 minutes following the wash step and incubated for 30 minutes at room temperature in the dark while gently shaking. The solutions turned from colorless to blue. Finally, the stop reagent (100  $\mu\text{L}$ ) is added into each well causing the solutions to turn from blue to yellow and the absorbance of each well is read immediately at 450 nm using a microplate reader. The optical density of the rhGH in 10% serum samples is plotted versus the concentration of each sample.

### **III.3 Results**

#### *III.3.1 Schematic Representation of Direct and Amplified SPRi*

The performance of SPRi and Nano-SPRi (SPRi employing NanoEnhancers) was compared with ELISA for the detection of rhGH in a complex environment. The differences in the setup of these methods are described here briefly. For SPRi (direct detection, Figure 3.1), the capture antibody is immobilized on the surface and then the sample is injected and binding of analyte to the sensor surface is measured directly in real time and label-free manner. However, with Nano-SPRi (Figure 3.1), after the analyte

binds to the sensor surface, a consecutive injection is followed with quantum dots coated with detection antibodies to amplify the SPRi signal. The ligands (rhGH or IgG specific antibodies) were immobilized in an array format on the SPRi biochip. Target protein (rhGh) spiked in human serum was introduced to the sensor surface are directly detected (SPRi) and sequentially highlighted with NanoEnhancers (Nano-SPRi).

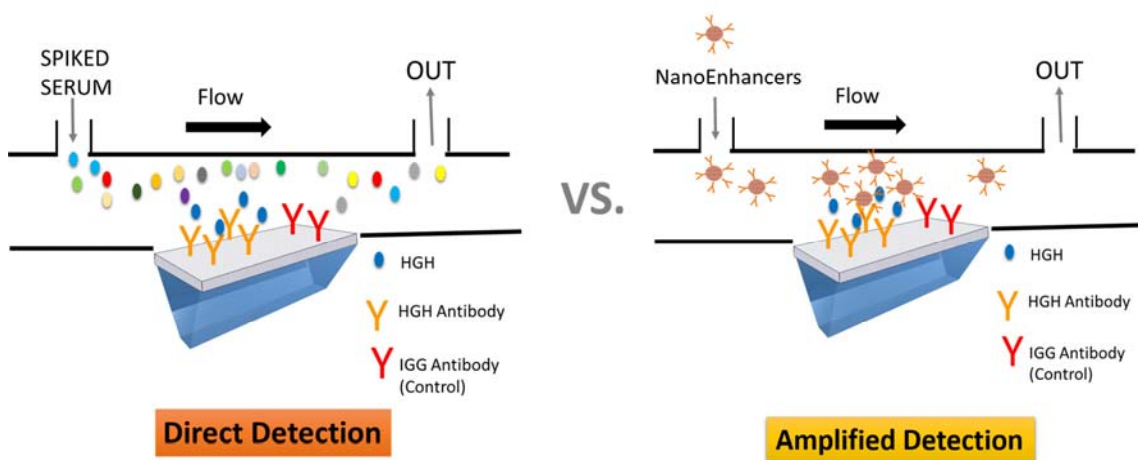


**Figure 3.1. A Schematic Representation Comparing Direct-Mode (SPRi) and Amplified-Mode.**

### *III.3.2 ELISA Setup and Analysis of RhGH in 10% Serum*

As for ELISA, the multiwell plates arrive already pre-functionalized with capture antibody and then the sample is introduced, the analyte of interest will bind. A detection antibody is introduced followed by substrate addition. The optical density is then measured at 450 nm. In this study, a commercial ELISA kit (Figure 2) was used to measure rhGH spiked in 10 % human serum.

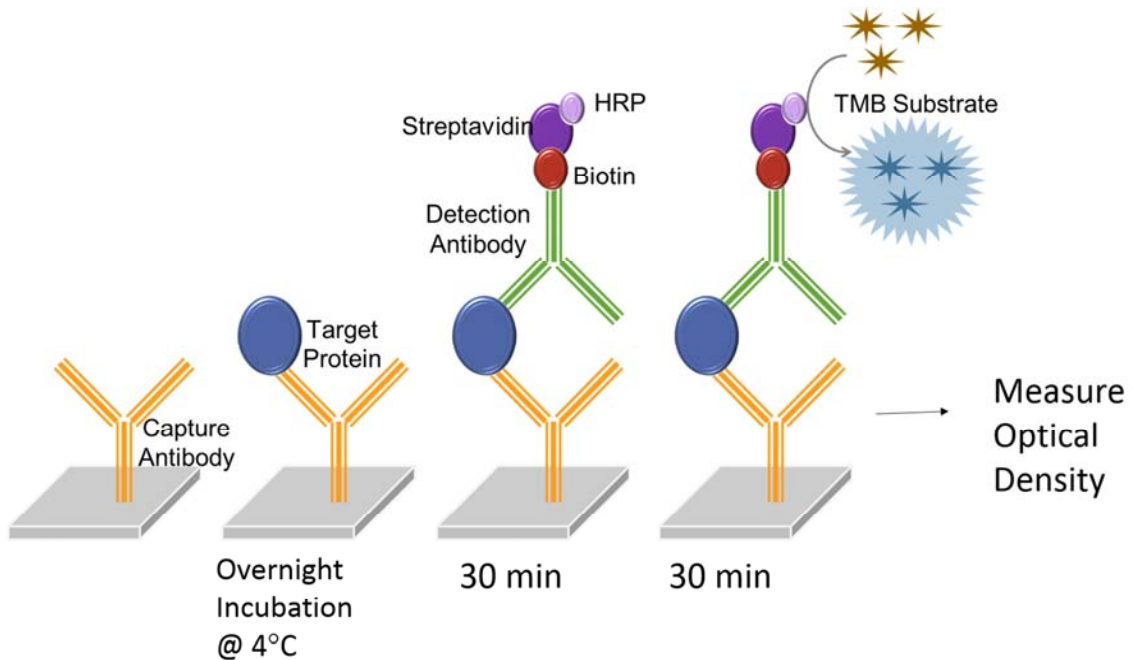


**Figure 3.2. A Schematic Representation of the ELISA Assay Procedure.** rhGH protein (blue ovals) is introduced to wells that have been pre-functionalized with monoclonal antibodies (yellow) specific to rhGH. Non-specific interactions are eliminated by rinsing the wells with wash buffer followed by the introduction of a detection antibody prefunctionalized with horseradish peroxidase (HRP, purple). The solution will change in color after adding the substrate tetramethylbenzidine (TMB, gold).

Figure 3.3 represents the titration curve of rhGH spiked in 10 % human serum and is plotted against the obtained OD at 450 nm. A good linear response was observed and the limit of detection was determined to be 1 ng/mL. The coefficient of variation (CV) was 6.5 % suggesting good reproducibility.

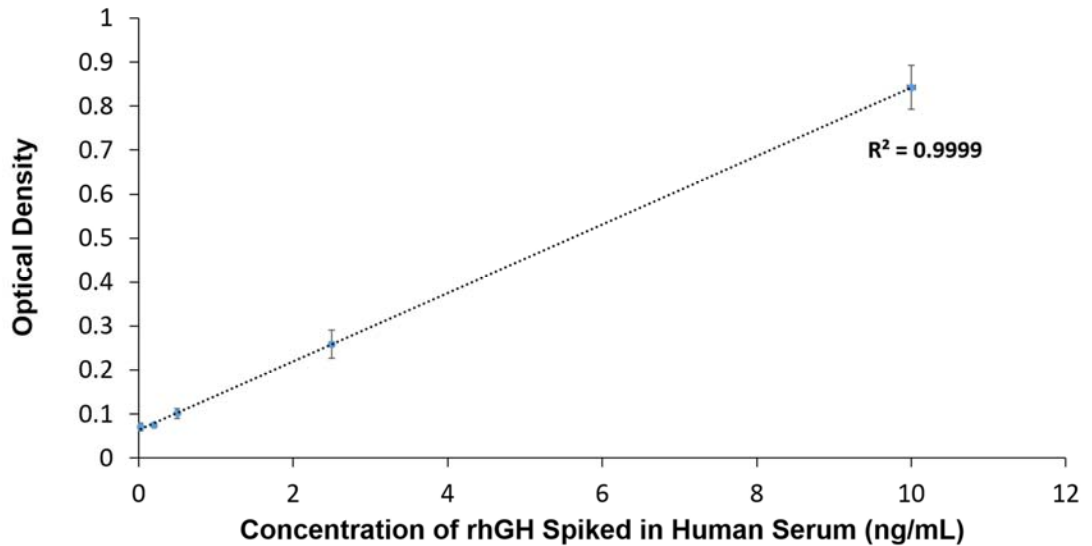


**Figure 3.3. ELISA Data Analysis. Concentration of rhGH spiked in serum is plotted against the obtained OD at 450 nm.**

### *III.3.3 Direct Detection of RhGH in 10% Serum with SPRi*

Next, the detection of rhGH spiked in human serum was assessed with SPRi. Direct detection of rhGH resulted with the corresponding concentration gradient curve (Figure 3.4), each point represents the average value of the reflectivity difference calculated from three SPRi kinetic curves for each concentration. The limit of detection (LOD) was determined to be 3.61 ng/mL. The SPRi direct detection assay was highly reproducible as the CV of the assay was only 4.1 %.

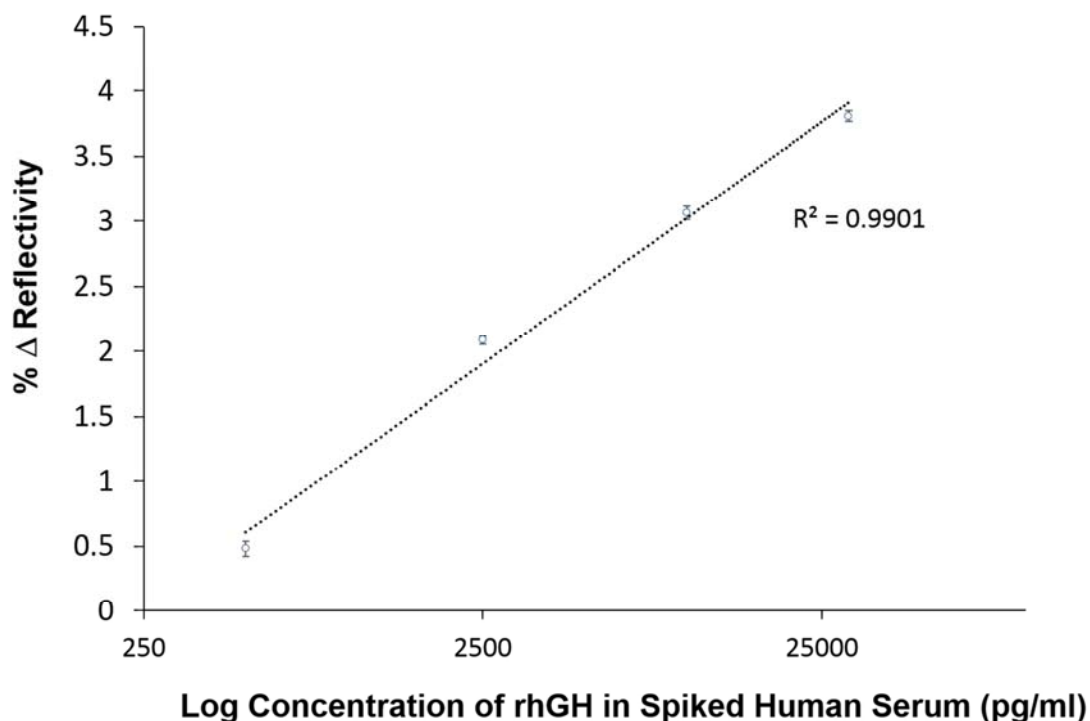


**Figure 3.4. Direct SPRi Detection of rhGH Spiked in 10 % Human Serum. The resultant normalized SPRi kinetic plot after the injection of various amounts of hGH spiked in human serum followed by the injection of a high salt buffer (dashed vertical line) to remove non-specific interactions. A concentration gradient curve representing the binding of various amounts of hGH spiked in human serum to the sensor surface that has been prefunctionalized with biotinylated hGH-specific-Antibody.**

#### *III.3.4 Amplified Detection of RhGH in 10% Serum with NanoSPRi*

To increase the sensitivity of the SPRi biosensor, NanoEnhancers (QDs pre-functionalized with detection antibodies) are sequentially introduced to the sensor surface in order to highlight the presence of rhGH spiked in human serum. After background subtraction, the NanoEnhancers were able to amplify the biosensor response up to 7.9 %, however, with minimal signal change (Immunoglobulin G (IgG)-specific antibody, 0.38

% change in reflectivity; Figure 3.5 on controlled regions of interest. Imaging of the sensor surface revealed that only regions of interest that have rhGH-specific antibodies immobilized experience the largest contrast change corroborating directly with the kinetic sensorgram response.

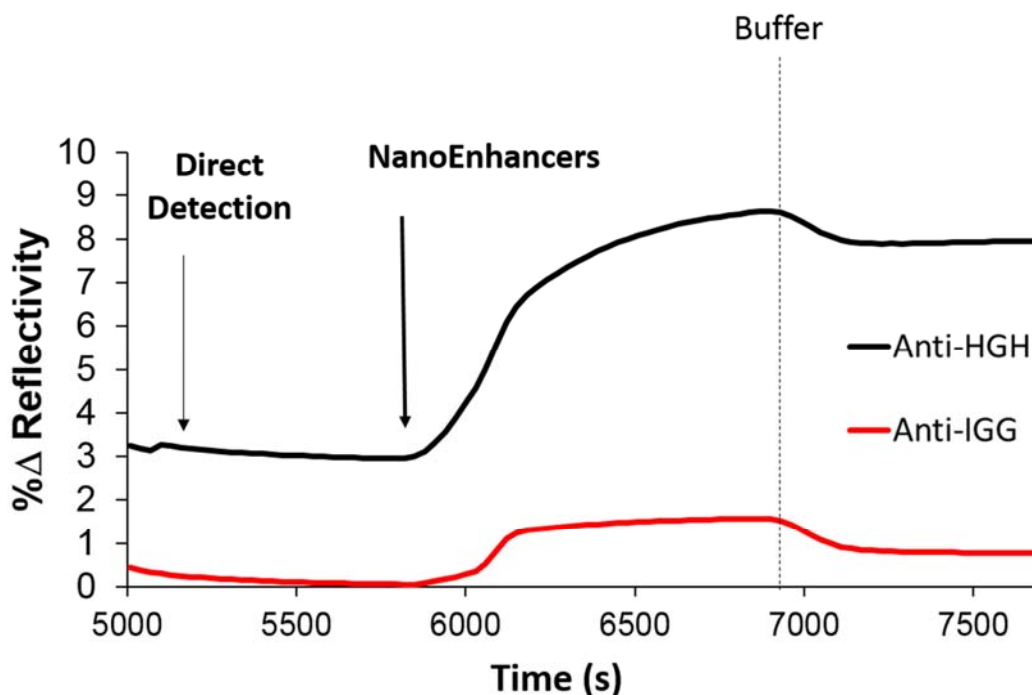


**Figure 3.5. Detection of rhGH Using a Sandwich Assay Spiked in 10 % Human Serum. SPRi kinetic plot after the injection of rhGH (30 ng/mL) in buffer (10 mM PBS, 150 mM sodium chloride, pH= 7.4) onto a pre-functionalized chip with 11-mercaptoundecanoic acid / rhGH-specific antibody and control IgG-antibody then blocked with BSA followed by the addition of detection antibody-coated quantum dots (NanoEnhancers).**

To demonstrate the practicability of the Nano-SPRi biosensor, the measuring range of rhGH in crude samples was assessed. An extended working range from 30,000 pg/mL to 0.25 pg/mL resulted as a response to the addition of NanoEnhancers (Figure

3.6). It is worth noting that each point on the titration curve is averaged from three independent experiments. Consequently, the lower limit of detection was calculated to be 9.20 pg/mL and the coefficient of variation was 20 %.

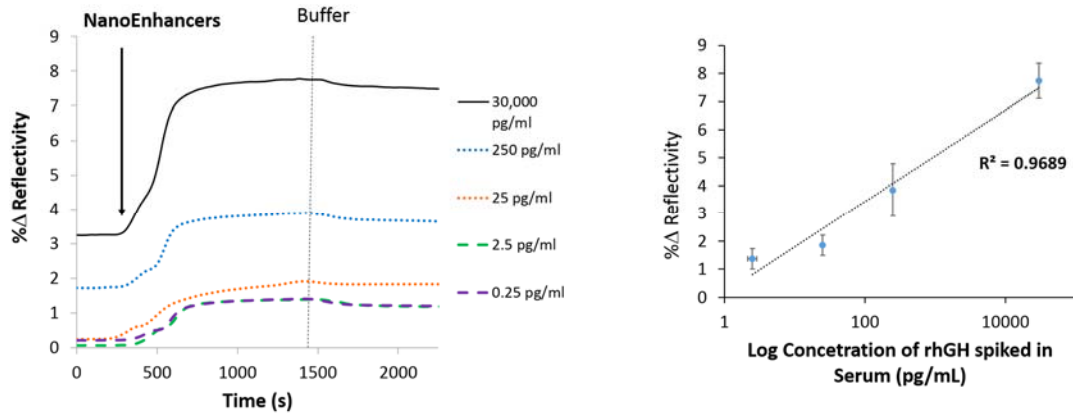


**Figure 3.6. Nano-SPRi Detection of hGH Spiked in Human Serum. Normalized SPRi kinetic plot representation of hGH\_specific\_Anti-QDs-amplified signal for human serum samples spiked with different concentrations of rhGH. A vertical dashed line (grey) represents the injection point of the running buffer. (b) A concentration gradient curve representing the binding of NanoEnhancers (hGH\_specific\_Anti-QDs) after the injection of various amounts of hGH spiked in human serum to the sensor surface that has been prefunctionalized with 11-mercaptoundecanoic acid /hGH-specific antibody.**

### III.3.5 Comparative Analysis of SPRi and NanoSPRi

Next, the change that occurs in the SPR reflectivity curve as a function of the concentration was compared between the direct and the NanoEnhancer bioassay method (Figure 3.7). For the direct detection technique between 25 and 0.25 pg/mL, the signal started to plateau and this is not surprising as these concentrations fall below the LOD of 3 ng/mL (Figure 3.7). Similarly, for the amplified technique, concentrations below the LOD of 9.2 pg/mL signal started to plateau and showed virtually no variation.

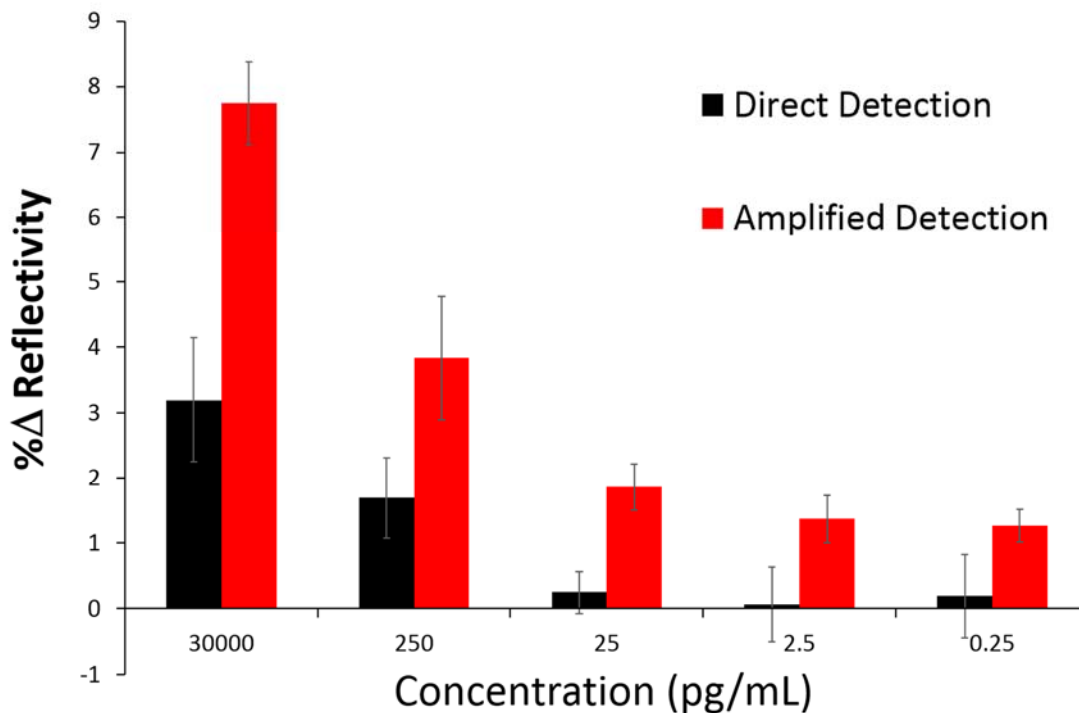


**Figure 3.7. A Comparative Analysis of SPRi with Nano-SPRi. This bar graph depicts the percent change in reflectivity (% $\Delta$ R) after introduction of rhGH spiked in human serum (direct detection) followed by the injection of NanoEnhancers (amplified detection) for 30,000 pg/mL, 250 pg/mL, 25 pg/mL, 2.5 pg/mL and 0.25 pg/mL.**

### *III.3.6 Specificity Analysis of NanoSPRi Platform*

Furthermore, the specificity of the Nano-SPRi biosensor was assessed. Insulin-like growth factor-1 (IGF-1) spiked in human serum was injected as a control since hGH stimulates the secretion of IGF-1 through the growth hormone receptor on the hepatocyte membrane. After the injection of the IGF-1 in serum, the NanoEnhancers were sequentially injected and the SPR signal response did not show any specific binding (Figure 3.8). However, when rhGH spiked in serum sample was injected to the very same

spot functionalized with rhGH antibody, signal enhancement was observed. In conclusion, the Nano-SPRi platform has demonstrated excellent specificity and selectivity for rhGH.

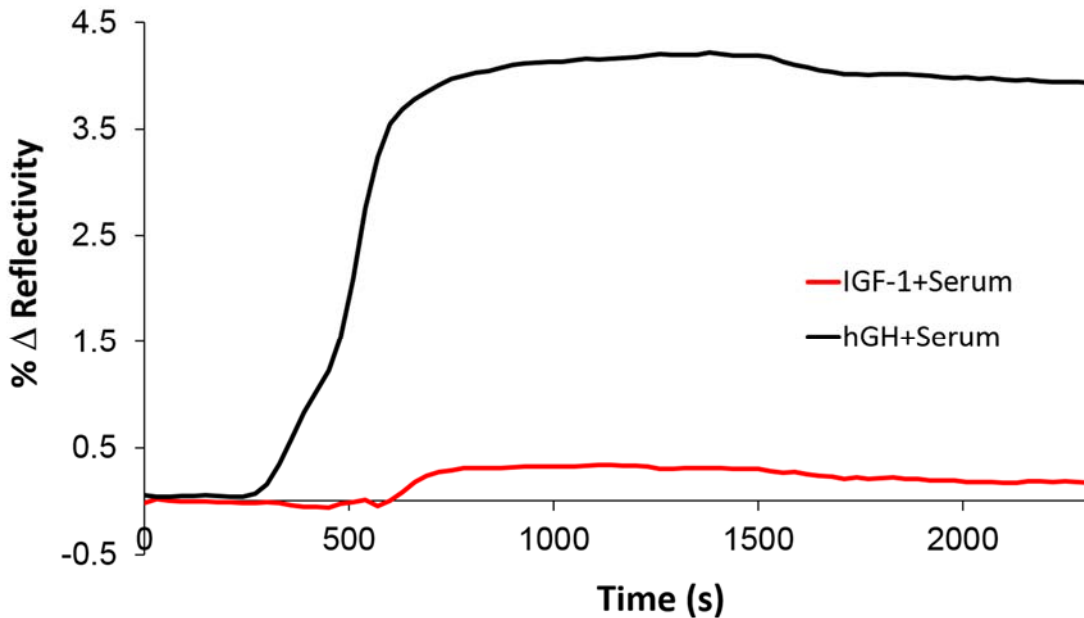


**Figure 3.8. Assessment of Nano-SPRi Selectivity to rhGH. The Nano-SPRi biosensor response after rhGH (black) and IGF-1 (red) are injected in spiked serum.**

### *III.3.7 Correlation Analysis Between ELISA and SPRi Results*

A correlation analysis was performed using the Pearson correlation coefficient to determine the correlation between the SPRi signal intensity and ELISA optical density values (Figure 3.9). A p-value < 0.01 was considered significant. As illustrated in this graph, there is a good correlation between the rhGH levels in spiked human serum measured by SPRi and ELISA. The r-value was 0.9263 for 9 different samples.

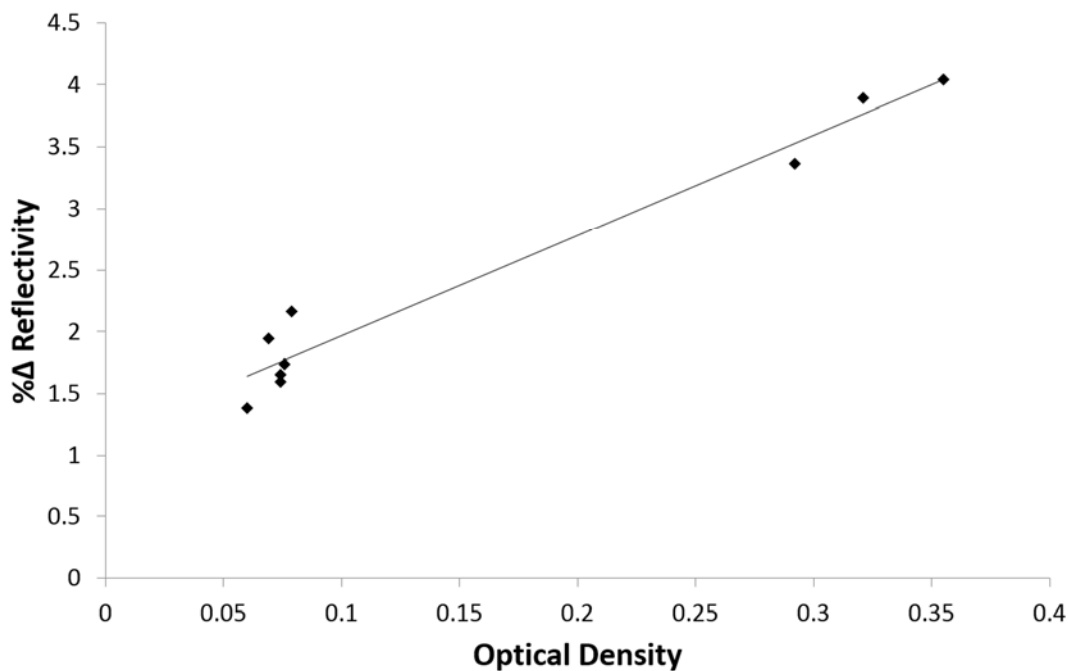


**Figure 3.9. Pearson Correlation Analysis Between ELISA and Nano-SPRi. The plot correlates Nano-SPRi signal intensity (y-axis) with ELISA optical density (x-axis) values. (Pearson correlation coefficient  $n=9$ ,  $r=0.9263$ ,  $p=0.00000183$ ).**

### *III.3.8 Kinetic Analysis of the Binding Event in ELISA and SPRi*

The equilibrium dissociation constant ( $K_D$ ) was determined using the graphpad software for ELISA. The calculated  $K_D$  value was approximately 79 nM (Table 3.3). The on ( $K_a$ ) and off ( $K_d$ ) rates could not be determined by ELISA. However, using the data analysis software, the direct detection method resulted with  $K_D$  value of 23 pM using the molecular mass of 22 kDa that corresponds to one rhGH molecule. The on and off rates were calculated to be  $6.1 \times 10^7 \text{ M}^{-1}\text{s}^{-1}$  and  $1.33 \times 10^{-3} \text{ s}^{-1}$ , respectively. This inherently translates that 0.13 % of the rhGH and antibody complexes decay per second. As for the

amplified SPRi experiment, a stronger overall interaction was observed between NanoEnhancers and rhGH as the calculated binding affinity was determined to be 4.3 pM. In addition, a stronger association rate was observed for NanoEnhancers and rhGH than capture antibody/rhGH, however the dissociation rate suggests that 0.26 % of NanoEnhancer/rhGH/Capture antibody decay per second.

**Table 3.3. Full Kinetic Data Analysis Including the Evaluation of the Affinity, On-rate and Off-rate of the Antibody Responses Using Graphpad (ELISA) and Data Analysis (SPRi and Nano-SPRi) Software. The determination of the avidity using the molecular mass of 22 kDa that corresponds to one rhGH molecule was chosen. The limits of detection were determined for all three studies using excel.**

Method	K <sub>D</sub> (Affinity)	K <sub>a</sub> (on-rate)	K <sub>d</sub> (off-rate)	LOD
ELISA	79.45 x 10 <sup>-9</sup> M	NA	NA	1 ng/mL
SPRi	23.2 x 10 <sup>-12</sup> M	6.1 x 10 <sup>7</sup> M <sup>-1</sup> s <sup>-1</sup>	1.33 x10 <sup>-3</sup> s <sup>-1</sup>	3.61 ng/mL
Nano-SPRi	4.33 x 10 <sup>-12</sup> M	7.54 x10 <sup>8</sup> M <sup>-1</sup> s <sup>-1</sup>	2.62 x10 <sup>-3</sup> s <sup>-1</sup>	0.0092 ng/mL

### III.4 Conclusions

Irregular levels of hGH, a naturally occurring hormone, have been linked to numerous medical disorders that affect human growth and development. Moreover, exogenous administration of rhGH is commonly used by athletes, even though it is forbidden, as a doping agent to enhance their performance. Challenges in detecting rhGH

misuse result from the difficulty in distinguishing exogenous hGH from endogenous form. As such, the current approved technique for detecting exogenous hGH relies on measuring the ratio of the 22 kDa hGH isoform in relation to the 20 kDa isoform. Since the isoform test demands for the measurement of multiple hGH isoforms simultaneously within a short period of time in a wide range of concentrations, therefore, we considered the SPRi platform as a perfect match. In addition, endogenous hGH level fluctuate to a very low level (0.03 ng/mL) in the bloodstream therefore the detection system must be able to measure this range comfortably with high specificity. As a result, we also investigated in this study the potential of Nano-SPRi as a diagnostic tool for hGH and compared it directly with SPRi and the classical immunoassay ELISA.

Based on results obtained from this study, the main advantage of the SPRi and Nano-SPRi method is that rhGH concentrations can be measured in a quicker manner in comparison to the more conventional method ELISA. A standard duration for measuring rhGH levels in one sample with the direct detection method was one hour whereas the Nano-SPRi required two hours due to the additional steps in the process. Overall, with SPRi and Nano-SPRi experiments, before the injection of a sample, a calibration step is highly recommended. In addition, the injection of a crude sample like human serum results in some non-specific interactions as a result it is imperative to inject a high salt wash buffer to only reveal specific interactions. It is also worth noting that a wash step is absolutely necessary after the introduction of blocking molecules to the sensor surface, to remove unbound molecules. As for ELISA time requirements are far greater (~16-18 h) for the analysis of one sample. A longer incubation time is needed as the sensitivity of the

assay is enhanced especially for this study, as the focus was to compare the lower limit of detection.

The choice of surface chemistry will vary from one application to another and this could be realized as one of the limitation of the SPRi technique. In this study, a wide range and combination of chemical linkers and blocking molecules were assessed to achieve the right combination in order to observe optimal binding efficiency of rhGH to the sensor surface. For example, in this study, the combination of BSA and PEG served well in minimizing non-specific interactions. However, in a previous study [71], where the capture ligand was an aptamers, PEG alone served as the best blocking molecule. The variables that affect binding efficiency of analyte to ligand are also dependent on pH, buffer and temperature. Therefore, with any application, these variables need to be optimized. In addition, it is critical to determine the optimal spotting concentration of the ligand to the chip surface. A titration experiment with a range of concentrations of immobilized ligands is performed before initiating the study. As for ELISA, a crucial step in the procedure was to decant the wash buffer from wells by tapping the microplate as this ensured no residual liquid is leftover. Removing the buffer wash with pipette was not sufficient as any residual liquid interfered with the signal reading of the target sample.

In reference to sensitivity, ELISA (1 ng/mL) is comparable to SPRi (3.61 ng/mL) but nano-SPRi (9.20 pg/mL) improves sensitivity by three orders of magnitude, thereby enabling measurements at the lower biological levels of rhGH 0.03 ng/mL. As we previously reported [55, 71], the signal enhancement imparted by the NanoEnhancers is attributed to a mass loading effect and the strong coupling that exists between NIR

fluorophores and propagating surface plasmons for gold film nanostructures. Even though, Nano-SPRi adds an extra step to the procedure, this level of sensitivity can widen the applications of SPRi technology in various outlets.

SPRi provides scientists a full kinetic profile ( $K_D$ ,  $K_a$  and  $K_d$ ) of antibody/rhGH interaction whereas ELISA can report only affinity values. The coefficient of variation (CV) was below 10 % for SPRi (4.1 %) and ELISA (6.5 %), suggesting good reproducibility. The ELISA and SPRi affinity values are different because the capture antibodies immobilized on the sensor chip are different from antibodies immobilized in the ELISA 96-well plate. As for Nano-SPRi a higher CV value (20 %) was observed. There are several parameters that can contribute as a source of errors for CV determination. For example, with the Nano-SPRi experiment a much lower concentration of analyte is being measured, the addition of NanoEnhancers adds another step in the procedure and the experiment was performed manually. A very good correlation between Nano-SPRi and ELISA was achieved for the detection of rhGh in spiked human serum. Finally, ELISA can be a reliable technique however the method itself is time consuming which makes it difficult to use in situations requiring real time monitoring and multiplexing, as it is the case with hGH. In addition, a more attractive feature that was not investigated directly in this study that SPRi offers over ELISA is the ability to measure hundreds of interactions simultaneously in real time.

In conclusion, this work presents Nano-SPRi as an ultrasensitive and accurate sensing platform for the detection of hGH biomarker in serum in comparison with conventional ELISA. Therefore in the next study, Nano-SPRi method will be assessed to

detect multiple biomarkers simultaneously in real time (multiplexing) at various concentrations in order to examine its potential as a viable clinical diagnostic tool. Furthermore, surface design will be improved to allow for a more reproducible immunosensor using an oriented method of antibody immobilization instead of direct covalent attachment. In addition, another hormone, progesterone, will be detected in the third work using Nano-SPRi. In this setup, the sensor surface is composed of x-aptamers immobilized on the sensor surface as the binding ligands specific for progesterone. This novel aptasensor is developed to offer the first label-free sensing assay capable of detecting progesterone in real-time and at very low concentrations (1 nM).

CHAPTER IV  
MULTIPLEX DETECTION OF ORGAN INJURY BIOMARKERS USING SPRI  
BASED NANO-IMMUNOSENSOR

**IV.1 Introduction**

Despite recent advances in targeted therapy and surgical care that have caused a drastic decrease in mortality rates, irreversible organ failure persists as the leading cause of high morbidity in critically ill patients [74, 75]. In most cases, the curative strategies fail to halt organ disease progression before reaching an irreversible stage due to a delay in the decision to begin treatment. The medical intervention decision often depends on clinical tests to observe for indicative biomarkers in bodily fluids. The development of such sensitive and non-invasive clinical assays not only will allow medical treatment at early stages; but also will enhance curative strategies, improve the quality of life and invoke better insight onto the mechanistic basis of organ injury.

Currently many analytical techniques with varying sensitivity and specificity have been developed and employed to detect clinical biomarkers; however, they are very limited in predicting disease progression at early stages. Mass spectrometry-based tools for example 2D/MALDI-MS and LC-MS/MS suffer from low sensitivity and require intensive data analysis done by professionals [76]. Immunoassays on the other hand such as enzyme linked immunosorbent assay (ELISA) are labor intensive, require frequent calibration, and are incapable of acquiring data in a high-throughput manner [77]. As for

nucleic acid based assays not only require complex hardware setup but also suffer from interference in some matrix types [78, 79]. Finally, in most of these assays, the degree of accuracy highly depends on the expertise of the pathologist. Hence, there is a lack of diagnostic tools that could accurately detect a panel of clinical biomarkers at the earliest time point possible and provide immediate results in a simple use manner and this presents itself to be the major impediment to treating organ injuries.

In the present work, an in vitro diagnostic optical assay based on surface plasmon resonance imaging (SPRi) is used to overcome the drawbacks of currently used tests to sensitively assess individual or multiple organ injury biomarkers at the same time. SPRi is a non-labeling and real time optical technique for the detection and analysis of biomolecular interactions at the surface of a high refractive index glass prism coated with a thin layer of metal. The sensing mechanism measures changes in refractive index up to ~ 300 nm from the metal surface. The surface plasmons are sensitive to refractive index changes occurring in the vicinity of the metal layer; hence, serving as the basis of the detection of biomolecular interactions.

Since the SPRi microarray platform allows for the quantitative detection of multiple interactions simultaneously better known as multiplexing, many studies have focused on this promising application to screen a variety of analytes in multiple matrices. For example, one group responded to the need of screening antimicrobial drug residues in milk due to their possible health risks by developing a competitive immunoassay for the simultaneous detection of seven drug residues down to ppb levels [80]. Others have extended multiplex sensing to low molecular weight protein biomarkers with clinical

significance in the body, such as  $\beta_2$ -microglobulin (MW=11.8 kDa) and cystatin C (MW=13.4 kDa) to reach nM limits of detection [81]. Multiple inflammatory cytokines (IL-1, IL-6, and TNF- $\alpha$ ) were also detected in saline buffer and cell culture medium at ng/mL levels to better serve in understanding disease diagnosis and progression [82]. Moreover, the parallel detection of cancer biomarkers in buffer and in blood samples has attracted much interest in a number of studies leading to the construction of robust and low-fouling assays with good sensitivity to improve current diagnostic tests [83, 84]. Therefore, excellent potential has been demonstrated by the novel list of microarray biosensors developed; however, sensitivity and reproducibility are key features that still demand improvements to meet the needs for clinical diagnostic analysis. Developing novel immobilization techniques that avoid alterations to the functionalities of biological receptors and adopting signal enhancers to decrease the limit of detection of biomarkers represent the areas where improvement can be applied for enhanced reproducibility and performance.

Hence, the work presented here introduces a dual microarray platform for the multiplex and ultrasensitive detection of two biomarkers, the High Mobility Group Box 1 (HMGB-1) and Kidney Injury Molecule-1 (KIM-1) biomarkers, which have shown potential prognostic value in acute liver disease [85-87] and acute renal failure respectively [88]. This platform incorporates specific capture antibodies for both biomarkers on the surface and NanoEnhancers (NIR quantum dots)-labeled detection to enable the ultrasensitive detection of biomarkers at 5 pg/mL (200 fM) concentrations. From our previous work, enhancing the sensitivity of SPRi was achieved using

NanoEnhancers independent of the type of capture ligand or analyte and even environmental conditions [55, 89]. Moreover, we will further improve the sensitivity of the immunosensor by immobilizing antibodies in a well-oriented manner to increase the reproducibility as well as sensitivity of the analytical measurements. Ultimately, the early detection of these biomarkers could provide detailed information on the evolution of the disease and assist in refining patient care.

## **IV.2 Methods**

### *IV.2.1 Materials and Chemicals*

Bare gold biochips were purchased from Horiba Scientific. Nanostrip was purchased from Cyantek (CA, USA). Protein A was purchased from protein mods (WI, USA). KIM1 and HMGB1 capture antibodies were purchased from abnova (Taipei, Taiwan). Biotinylated HMGB1 detection antibody was purchased from abnova and KIM1 detection antibody was also purchased from abnova and was functionalized with biotin using the biotinylation kit purchased from VWR (PA, USA). The fc fragment was purchased from EMD Millipore (MA, USA). Rabbit IgG polyclonal antibodies, polyethylene glycol (PEG2000), and bovine serum albumin (BSA) were purchased from Sigma Aldrich (PA, USA). Phosphate buffered saline (PBS) tablets and D (+)-Sucrose were purchased from fisher scientific (PA, USA). Streptavidin coated near infrared quantum dots (NIR-QDs) were purchased from life technologies (NY, USA).

### *IV.2.2. Sensor Surface Preparation*

The bare gold biochip was cleaned using a nanostrip solution (under sonication for 90 mins, 50°C) and then rinsed thoroughly with deionized water, dried with a stream

of Nitrogen and placed in the UV/Ozone for 5 mins prior to surface functionalization. Protein A (5  $\mu\text{g/mL}$ ) was immobilized on the surface of the biochip and incubated for 4 hours at room temperature and a relative humidity of  $\sim 75\%$ . Following this step, capture antibodies specific for KIM-1 (50  $\mu\text{g/mL}$ ), HMGB-1 (50  $\mu\text{g/mL}$ ) as well as Rabbit IgG antibodies (50  $\mu\text{g/mL}$ , negative control) were deposited on the surface (500  $\mu\text{m}$  spots) using a LabNext Microarrayer system. This spotting system prints the antibodies in an orderly and systematic manner on the sensor chip using a 500  $\mu\text{m}$  Teflon pin. It is important to note that both KIM-1 and HMGB-1 antibodies along with the negative were attached to the surface in the multi-target sensor surface design; however, only one type of antibody with the negative control was immobilized in the individual biomarker detection measurements to determine the limit of detection.

The biochip was then allowed a 2-hour incubation time for efficient immobilization at room temperature and relative humidity of 75%. Prior to SPRi measurements, the functionalized surface was blocked inside the instrument using a combination of PEG2000 (2 mM) and BSA (1%) sequentially injected above the sensor surface.

#### *IV.2.3. SPRi Measurements*

The analysis of biomolecular interactions of the different capture ligands with the corresponding biomarkers was performed in a Horiba SPRi-PlexII model (Horiba Scientific, France) designed particularly for multiplexing purposes. The biochip was loaded into the hexagonal flow cell (11  $\mu\text{L}$  capacity) inside the instrument and a running

buffer (10 mM PBS, PH=7.4), controlled at a rate of 20  $\mu$ L/min by a continuous flow syringe pump (Harvard Apparatus PHD 2000 Infusion), was flown over the surface. Specific spots of each capture antibody (24 spots, 400  $\mu$ m diameter each) were selected and defined using the SPRi view software. The sensing mechanism utilized a high stability LED incident light source that hits the glass prism coated with 5 nm Chromium adhesion layer and 50 nm gold, a detector that collects the resulting reflected light and a CCD camera that provides a real-time digital contrast image of the sensing surface. This image component reflects the biomolecular binding events happening at the metal surface; hence, confirming the changes in reflectivity in the SPRi response. Bright areas on the surface represent a binding event and dark spots are vice versa.

Prior to kinetic monitoring, the surface was sequentially blocked by the injection of PEG2000 (2 mM) and BSA (1%) prepared in the running buffer. This is followed by a calibration procedure involving the injection of sucrose (3 mg/mL) above the surface to account for buffer changes in all ligand spots on the surface. The flow rate was then slowed down to 10  $\mu$ L/min and allowed to equilibrate prior to the interaction measurements. This is done to permit an increased interaction time between the biomarker and the capture antibody until the detection and amplification probe are introduced to the surface.

The kinetics of the biomolecular interactions was monitored through the sequential injection of the biomarkers, fc fragment, biotinylated detection antibodies and finally the NIR-QDs for signal amplification. Each injected sample was prepared in the running buffer at room temperature. The fc fragment was introduced after the biomarkers

to avoid any possible steric hindrance blocking the antibody-binding site from reacting with the biomarker of interest. The introduction of biotinylated detection antibodies served to bind to the analyte on one hand and to the streptavidin coated NIR QDs through the strong biotin/avidin non-covalent interaction on the other hand.

The SPRi response reported is the average response of 4 spots of each capture antibody on the surface with the non-specific (negative control) signal subtracted.

### **IV.3 Results**

#### *IV.3.1 Biosensor Surface Optimization*

The overall performance of the SPRi biosensor highly depends on the quality of the surface functionalization and the proper anchoring of the biorecognition probes onto the metal surface. Most gold surfaces are functionalized by alkanethiol organic compounds as the primary building blocks onto which the biological ligands are covalently bound. For example, the immobilization of antibodies in immunoassays can be performed by the amine coupling of lysine residues in antibodies to the surface linked carboxylic acid groups through an EDC/NHS intermediate activation step. This surface chemistry has been widely used and successful in many previous works [90-92]; however, we found this strategy to be characterized by inconsistency in surface uniformity from one experiment to the other as shown (Figure 4.1). Therefore, we chose to design the capture array by immobilizing the KIM-1 and HMGB-1 monoclonal capture antibodies onto a protein A coated surface to avoid structural alterations to the antibodies, ensure proper orientation of the antibody and uniform coverage on the surface [93]. We found that coating the surface with protein A (5  $\mu\text{g/mL}$ ) solution for 4 hours enabled a

homogeneous coverage and active binding of the capture antibodies spotted on the surface, which enhanced the sensitivity and reproducibility of the SPRi response.

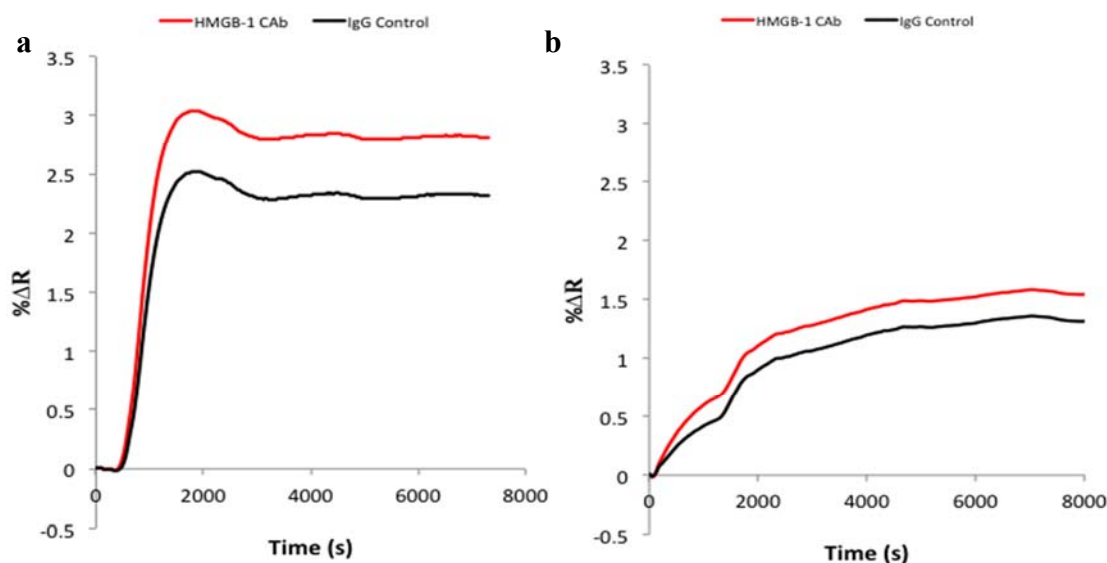


**Figure 4.1. Comparative Biosensor Behavior in Response to HMGB-1 (4  $\mu\text{g/mL}$ ) in Buffer. Both experiments A and B were carried out under the same conditions and prepared using the alkanethiol/EDC/NHS surface onto which the HMGB-1 monoclonal capture antibodies were covalently bound (amine coupling). Experiment (a) resulted in a low specificity signal of  $\Delta R = 3\%$ ; while experiment (b) gave a lower and inconsistent response of  $\Delta R = 1.5\%$ .**

#### *IV.3.2 Minimizing Non-Specific Interaction*

A well-designed immunoassay sensor not only relies on the proper immobilization of the biological ligands but also on the suppression of non-specific adsorption of analyte on the metal surface. And the challenge lies in choosing a blocking

agent of suitable dimensions and properties that can minimize the potential of non-specific signal but at the same time allow accessibility to the binding site of the bioreceptor. In this study we found that the sequential blocking using 2 mM polyethylene glycol (PEG2000) and 1% bovine serum albumin (BSA) provided optimal coverage of the surface against non-specific adsorption of analyte. The concentrations used were critical as increasing the concentration of PEG2000 from 0.1 mM to 2 mM while keeping the BSA concentration at 1% as well blocking the surface with proper sequence, enhanced the signal significantly from (1.7%  $\Delta R$ ,  $\pm 0.18$ ) to (3.45 %  $\Delta R$ ,  $\pm 0.08$ ), as shown in Figure 4.2. In addition, the protein A coated surface was further blocked by fc fragments (0.5  $\mu\text{g}/\text{mL}$ ) after injection of biomarker in order to occupy the free protein A regions not bound to the immobilized antibodies. Hence, with the combination of multiple agents, we were able to reach a negligible non-specific binding signal allowing our platform to perform successfully in the multistep sensing mechanism.

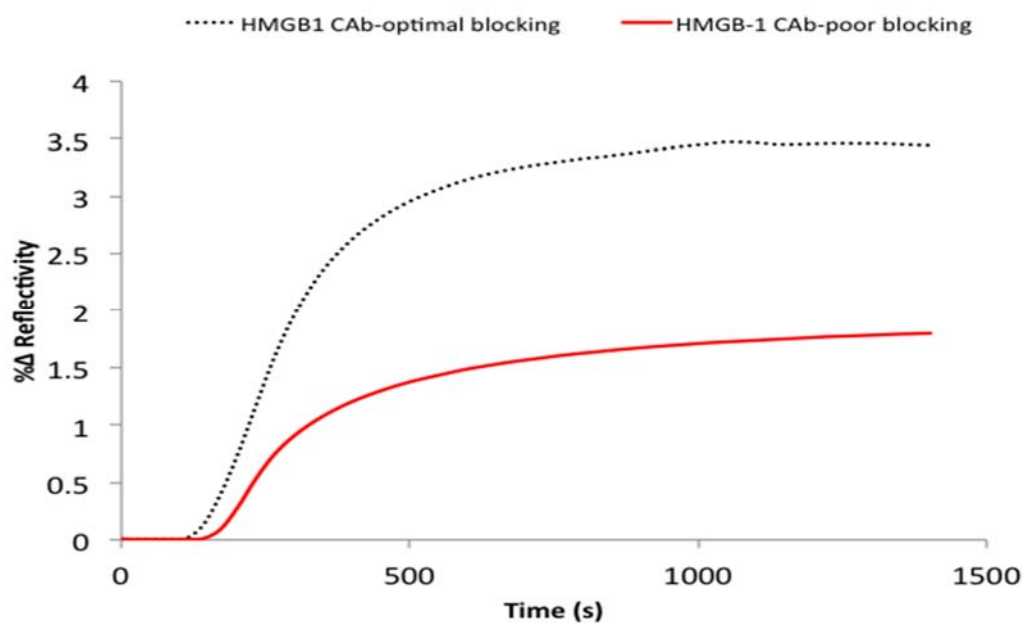


**Figure 4.2. Comparative SPRi Sensorgrams to HMGB-1 Binding to Two Surfaces Under Different Blocking Conditions. Above figure represents the binding kinetics of HMGB-1 (50 ng/mL) to two surfaces functionalized with HMGB-1 capture antibodies (50  $\mu\text{g/mL}$ ) and blocked under two conditions. The first surface was blocked using a combination of 0.1 mM PEG2000 and 1% BSA resulting in a signal of 1.7%  $\Delta\text{R}$ ,  $\pm 0.18$  (red solid line). While the second surface was blocked using a combination of 2 mM PEG2000 and 1% BSA and the binding of HMGB-1 resulted in a signal of 3.45 %  $\Delta\text{R}$ ,  $\pm 0.08$  (black dotted line).**

#### *IV.3.3 Singleplex Measurements of KIM-1 and HMGB-1*

A sandwich assay was used to detect KIM-1 and HMGB-1 separately at low concentrations in buffer. The capture array was first coated with protein A (5  $\mu\text{g/mL}$ , 4 hours) and then monoclonal KIM-1 and HMGB-1 antibodies and rabbit monoclonal IgG antibodies (negative control) were directly attached to the surface at 50  $\mu\text{g/mL}$  spotting concentration. The functionalized biosensing surface was then blocked using a

combination of BSA (1%) and PEG2000 (2 mM) inside the instrument. The detection of biomarkers was accomplished in a three-step process.

At first, the biomarker was injected and followed by sequential injection of the fc fragment to block the unoccupied protein A bound to the sensing surface. Secondly, specific biotinylated KIM-1 detection antibodies were injected to bind to the captured analyte. Finally, the signal amplification was accomplished with a non-interfering streptavidin coated NIR quantum dot (NanoEnhancers). The introduction of NIR quantum dots in the amplification process is known to lead to signal amplification due to the mass loading effect of the nanoparticles and possible emission coupling with the oscillating surface plasmons on the metallic surface [55].

A concentration range (0.005, 0.05, 10, and 50 ng/mL) of HMGB-1 biomarker in phosphate buffer was detected and the specific SPRi responses obtained are presented in (Figure 4.3). Secondly, a concentration range (0.005, 0.05, 0.5, and 50 ng/mL) of KIM-1 biomarker was tested and the results of the SPRi response are shown in (Figure 4.4). From these plots we were able to calculate the limit of detection for both biomarkers to be 5 pg/mL.

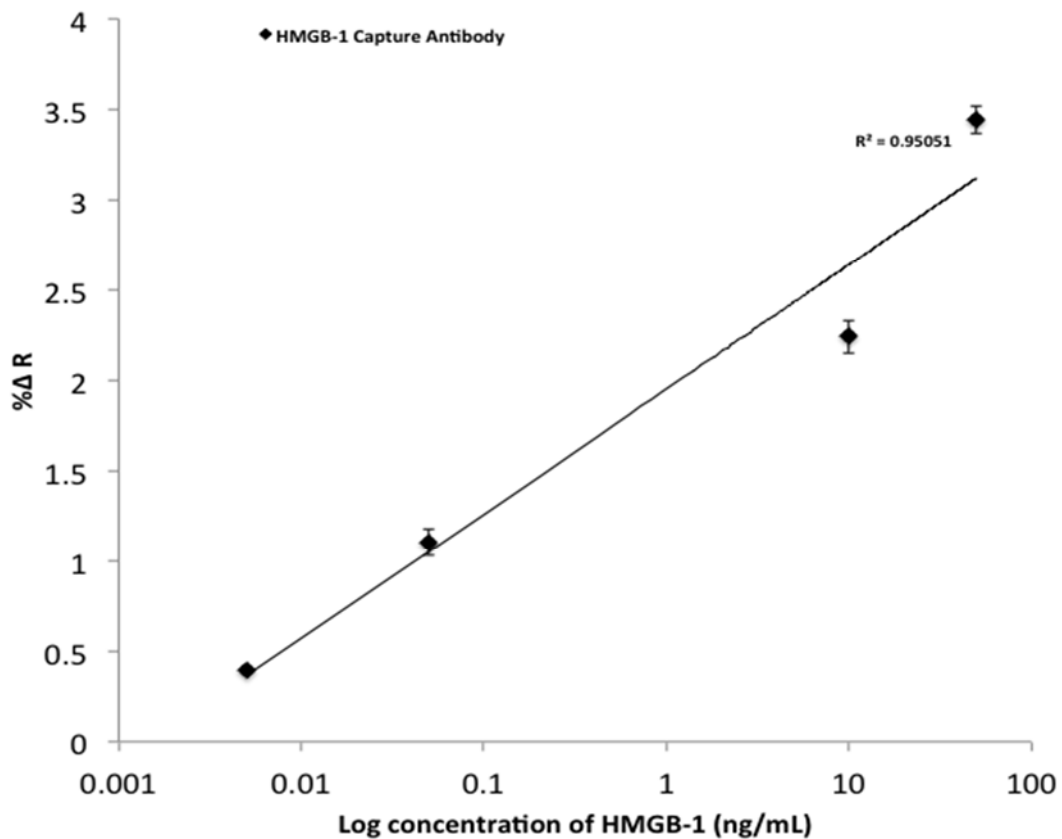


**Figure 4.3. A Concentration Profile of Nanoenhanced SPRi Signal in Response to HMGB-1 in Buffer. SPRi response (%Δ Reflectivity) represents the NanoEnhanced response upon the binding of NanoEnhancers to the various concentrations of HMGB-1 biomarker (ng/mL) in phosphate buffer. The % change in reflectivity reported takes into account the IgG negative control signal, which is subtracted from the overall signal.**

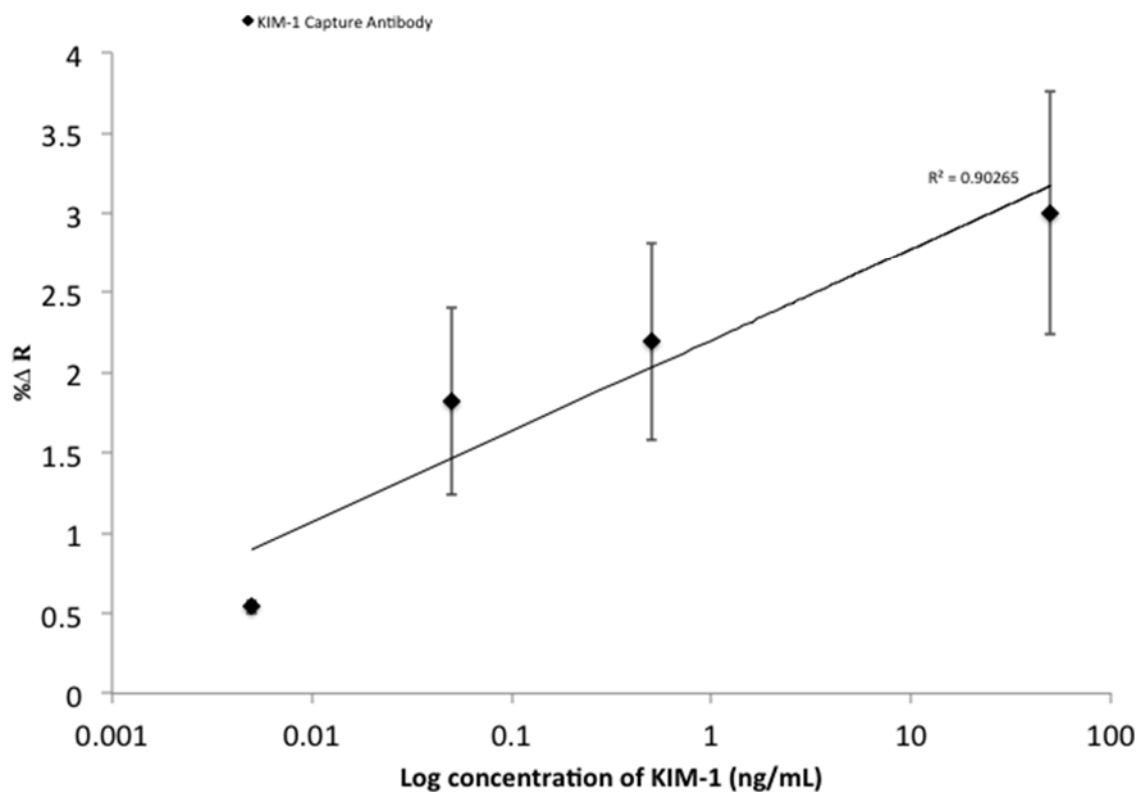


**Figure 4.4. A Concentration Profile of Nanoenhanced SPRi Signal in Response to KIM-1 in Buffer. SPRi response (%Δ Reflectivity) represents the NanoEnhanced response upon the binding of NanoEnhancers to the various concentrations of KIM-1 biomarker (ng/mL) in phosphate buffer. The % change in reflectivity reported takes into account the IgG negative control signal, which is subtracted from the overall signal.**

#### *IV.3.3 Multiplex Measurements of Both KIM-1 and HMGB-1*

To further investigate the multi-target potential of this biosensing platform, both KIM-1 and HMGB-1 antibodies along with the negative rabbit IgG control were spotted on the same surface at 50 μg/mL concentrations. The multiplex detection involved a three-step sandwich assay process very similar to the individual biomarker detection previously presented. The first step involved the injection of both biomarkers in buffer

followed by injection of fc fragment (0.5  $\mu\text{g}/\text{mL}$ ) to further block the unoccupied protein A regions. The second step introduced the biotinylated KIM-1 detection antibody and finally the NIR streptavidin-coated QDs were injected as the amplification probes (Figure 4.5).

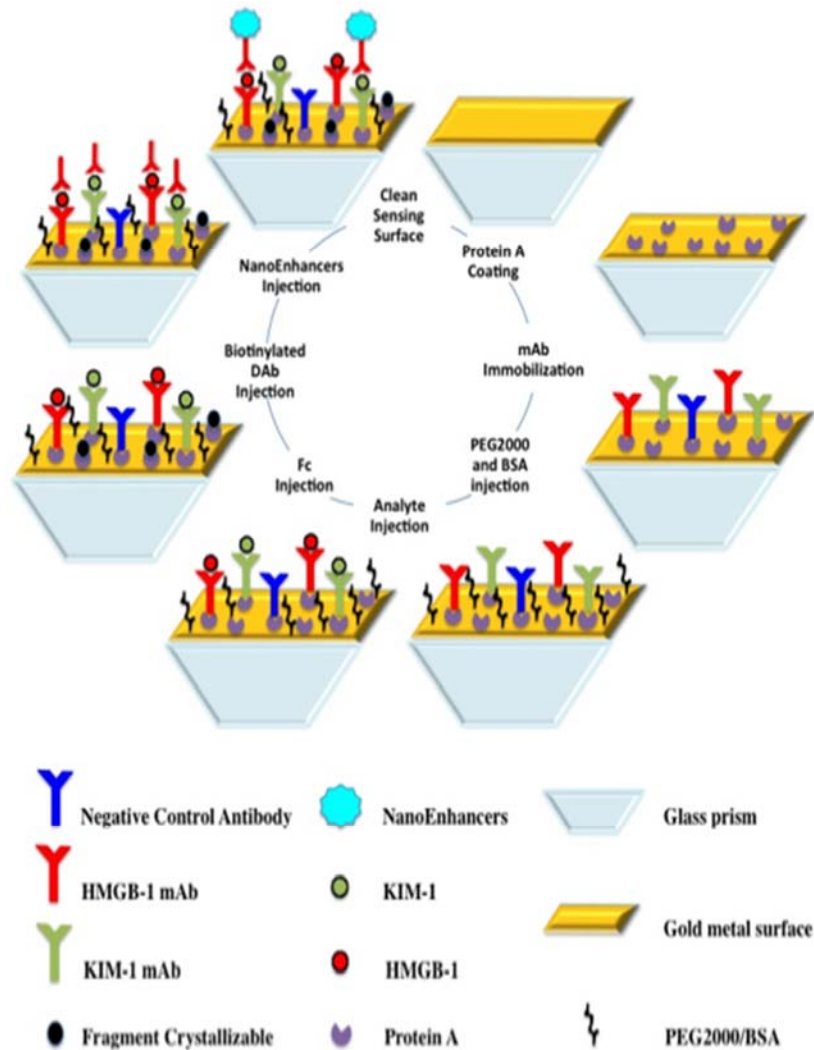


**Figure 4.5. The Step-Wise Experimental Approach in the Design of Sandwich Assay.** The setup demonstrates the sequential steps performed to design the immunosensor surface as well as to carry out the multiplex measurements of both KIM-1 and HMGB-1 biomarkers. Firstly, a clean surface is coated with protein A, followed by the immobilization of monoclonal antibodies, and then the surface is blocked with a combination of PEG2000 and BSA. The multiplex measurements are carried out by the sequential injection of biomarker, fc, biotinylated secondary antibody and finally NanoEnhancers to amplify the signal.

The results of the multiplex sandwich-amplification assay that detects HMGB-1 (0.5 ng/mL), KIM-1 (50 ng/mL) and IL-6 negative control (50 ng/mL) are presented in Figure 4.6. The SPRi response is highest for the KIM-1 biomarker ( $\sim 2\% \Delta R$ ,  $\pm 0.64$ ), and lower for the HMGB-1 biomarker ( $\sim 0.9\% \Delta R$ ,  $\pm 0.12$ ), with a negligible signal for the IL-6 negative control.

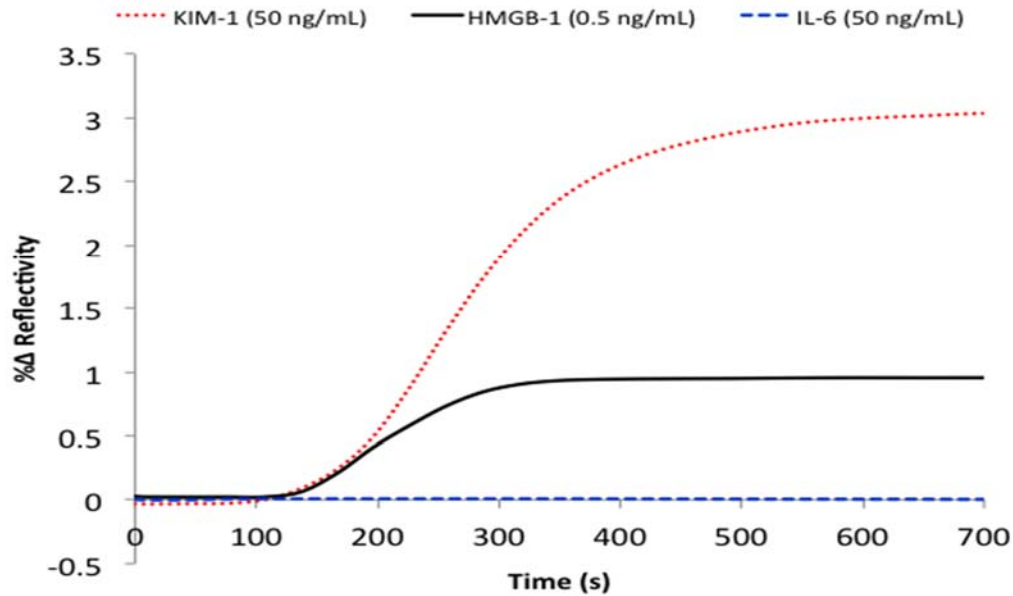


**Figure 4.6. Multiplex SPRi Sensorgram of KIM-1, HMGB-1 and IL-6 Control. The sensorgram represents the Nanoenhanced SPRi response (% $\Delta$  Reflectivity) versus time (s) of 50 ng/mL KIM-1 biomarker (dotted red line), 0.5 ng/mL HMGB-1 biomarker (solid black line), and 50 ng/mL IL-6 control (dashed blue line) measured in phosphate buffer.**

#### IV.4 Conclusions

We adopted a non-covalent attachment setup to immobilize the capture antibodies onto the sensing surface in order to avoid inconsistent results and enhance the reproducibility of the assay [93]. The inconsistency resulting from the chemical attachment of antibodies could perhaps be caused by the disordered orientation of the capture probes on the surface, which in turn could lead to loss of biological activity and hindrance in the analyte accessibility onto the binding site [94]. Protein A was bound to the sensing surface as the primary building block through the thiol-gold bond onto which

the antibodies will be spotted. Protein A is mainly used in antibody-purification columns as it binds to the fragment crystallizable (Fc) region of the antibody leaving the antibody-antigen binding site (Fab) accessible to bind to the biomolecule. An optimal density of protein A (5  $\mu\text{g/mL}$ ) and a spotting concentration of the capture antibodies (50  $\mu\text{g/mL}$ ) were utilized in the platform to ensure exposure of the binding site of the antibody and a sterically favored distance between the assembled antibodies. As a result, the sensing capability of the assay was enhanced and showed good reproducibility.

Moreover, functionalizing the surface with non-fouling materials took many attempts prior to finding the proper combination as well as concentration. It is important to note that this surface design allows more exposure to the bare gold metal surface than surfaces covered with alkanethiol groups in the layer below the antibodies. Therefore, blocking with PEG2000 chains allowed (2 mM) coverage of the areas between the spotted antibodies through the thiol-gold bond as well as the rest of the sensor chip. Additionally, blocking with BSA (1 %) was performed to offer extra protection as a coating layer to the protein A regions that were not occupied with antibodies. Since this surface setup is used for the first time in multiplex sandwich-amplification assay, a further non-specific adsorption challenge arose from the possible binding of the biotinylated complementary detection antibodies to the protein A. Therefore, to avoid that problem, Fc was injected to occupy the remaining unoccupied protein A sites. Furthermore, the injection occurred after the injection of the analyte in order to prevent any steric hindrance that Fc might cause to the binding site of the capture antibodies.

Finally, with all the surface development steps accomplished, singleplex detection for both HMGB-1 (~29 kDa) and KIM-1 (30 kDa) was performed in a sandwich-amplification assay achieving a limit of detection of 5 pg/mL (200 fM) for both biomarkers. This high level of sensitivity was accomplished by the addition of the NanoEnhancers resulting in superior sensitivity and limits of detection compared to reported values from currently exploited detection tools as it is highly important to detect these biomarkers at early stages [95]. For example, a LOD of 10 ng/mL in serum for HMGB-1 was achieved utilizing a combination of aptamer nanotechnology and electrophoresis [96], and a LOD of 2 ng/mL in an ELISA assay performed to selectively detect HMGB-1 in serum [97]. On the other hand, KIM-1 was detected using an immunochromatographic assay at concentrations higher than 800 pg/mL [98]. A further contribution to obtain more insight on disease detection and progression is accomplished by the multiplex sandwich-amplification assay that detects HMGB-1 (0.5 ng/mL) and KIM-1 (50 ng/mL) simultaneously to yield a higher signal for the KIM-1 biomarker (~2%  $\Delta R$ ), a lower signal corresponding to the HMGB-1 biomarker (~0.9 %  $\Delta R$ ) as expected, and a negligible signal for the IL-6 negative control. From these results, we can conclude that the platform demonstrates specificity and selectivity.

The enhancement in SPRi signal caused by the addition of the NanoEnhancers to the sensing surface could perhaps be caused by multiple reasons. The NanoEnhancers are heavy metal nanoparticles that result in a high mass loading effect responsible for the increased SPRi response. In addition, the NIR quantum dots possess unique quantum

properties, which could possibly allow energy coupling with the gold metal layer on the surface as reported in one previous study [55].

In this article, we propose a real-time, label-free, and multiplex nanoenhanced SPRi platform to quantitatively assess two biomarkers, kidney injury molecule (KIM-1) and high mobility group box-1 (HMGB-1) simultaneously in buffer. Our work involves three major contributions in the design of the immunosensor: (1) we applied site-specific immobilization of antibodies to the solid surface that avoids loss of biological activity obtained with covalent attachment; (2) we constructed a well-blocked sensor surface that experiences minimal non-specific adsorption for singleplex measurements of each biomarker in buffer; and (3) we adopted a sandwich assay that implements functionalized quantum dots (NanoEnhancers) as signal enhancers to achieve a sensitivity level of 5 pg/mL for KIM-1 and HMGB-1 in buffer. We foresee great potential and success in extending this multiplex and ultra-sensitive platform to assess a variety of other emerging clinical biomarkers at low concentrations and in complex matrices.

In future work, the proposed platform can be further investigated for the analysis of a vast number of different biomarkers simultaneously and in a variety of complex matrices. Furthermore, potential adjustments to the platform can advance the multiplex effectiveness of the technique to not only assess biological molecules and organ injury biomarkers; but also environmental toxins, microbes, drugs and many more. Therefore, we anticipate great contribution from the practical capabilities of this platform to medical, pharmaceutical and environmental research.

CHAPTER V  
ULTRASENSITIVE DETECTION OF PROGESTERONE USING A NANO-SPRI  
BASED APTASENSOR

**V.1 Introduction**

Steroid hormones are a family of small hydrophobic analytes derived from cholesterol that have been the targets in many clinical assays being developed for the detection of steroid hormones in a variety of bodily fluids and at very low concentrations [99]. Progesterone, a steroid hormone composed of four cyclic hydrocarbons containing oxygenated functional groups such as ketones, serves as an indicator of early pregnancy, and participates in controlling hormonal levels throughout the reproductive cycle. Its sensitive detection in diverse matrices can assist in fertility investigations [100, 101]. Progesterone normally ranges in level from less than 1 ng/ml serum in the pre-ovulation phase of the menstrual cycle up to 20 ng/ml in mid cycle, and to 300+ ng/ml in pregnancy. Immunoassays such as ELISA [102], electrophoresis-chemiluminescence detection [103], and non-competitive idiometric or fluoroimmunoassays [104], have been the most widely used methods for the detection of progesterone in different matrices. These tests require very carefully operated procedures, skilled experts to carry out the analysis, and labeled probes to detect the steroid. In addition, the major drawback of these

clinical tests is the high levels of interference arising from the structural similarities of the different hormones [99]. SPRi biosensor technology offers a reliable analytical tool to generate accurate and label-free signal detection of progesterone, real-time data acquiring, and semi-automated operation. This potential platform has been utilized to measure progesterone by employing well-developed immunoassays that utilize monoclonal antibodies as the binding ligands and sensitive surfaces. For example, an inhibition immunoassay procedure was adapted for measuring progesterone levels in cow's milk and human saliva to achieve a limit of detection of 3.5 ng/mL [105] and by further varying a number of parameters the same group was able to enhance the sensitivity down to 0.4-0.6 ng/mL in milk and 35-60 pg/mL in HBS-EP buffer [101]. Another study evaluated progesterone conjugated to different length ovalbumin linkers to determine the effect of these linkers on the anti-progesterone binding activity to achieve a sensitivity range from 0.1-50 ng/mL [106]. Signal enhancement probes such as gold nanoparticles were also investigated for their potential to detect progesterone conjugated to ovalbumin to lower the limit of detection to 4.9 ng/L in an inhibition immunoassay [107]. A similar platform was developed by Mitchell *et al.*, which consisted of immobilizing progesterone on the surface with oligoethylene glycol linkers and gold-streptavidin labels to lower the detection limit to 8.6 pg/mL [108]. As concluded from the studies reported, the SPR systems have been capable of providing a successful means of detection for progesterone. Nevertheless, the use of monoclonal antibodies as the capture ligands continues to pose an obstacle for sensitive, rapid and reproducible detection of progesterone. Most of the studies presented utilized an inhibition immunoassay, which required additional

preparation and use of larger amounts of antibodies prior to analysis; whereas a direct detection platform eliminates this additional step. Moreover, most of the detection strategies relied on modifying progesterone with linkers for immobilization to the sensor surface due to the small size of progesterone and its hydrophobic properties. This conjugation strategy can possibly alter the three-dimensional structure of the hormone and cause steric hindrance; hence, decreasing the sensitivity and reproducibility of the analytical measurements.

In this work, we introduce the use of progesterone x-aptamers as an alternative to monoclonal antibodies used in immunoassays for the ultrasensitive detection of progesterone in buffer. The setup that we adopt eliminates the need to covalently immobilize progesterone to the solid metal surface; hence, preserving the activity and steric accessibility of progesterone.

We also aimed to enhance the small molecule sensing by using a SPRi NanoEnhanced sandwich assay to allow for ultrasensitive detection of progesterone. Aptamers are short single-stranded oligonucleotide sequences, which mimic antibody binding to an analyte such as progesterone but with an enhanced sensitivity, specificity, and affinity. [109]. Furthermore, the use of aptamers may circumvent the problems of steric hindrance that occur between small molecules and large antibodies and which can decrease the sensitivity of the detection platform [110-112].

## **V.2 Methods**

### *V.2.1 Chemicals and Materials*

Bare gold chips were purchased from Horiba Scientific (France). Nanostrip was purchased from Cyantek (CA, USA). 11-mercaptoundecanoic acid, N-Hydroxysuccinimide, Poly (ethylene glycol) methyl ether thiol (Mw=800) and Poly (ethylene glycol) methyl ether thiol (Mw=2000), extravidin, glycerol,  $\beta$ -estradiol and acetonitrile were all purchased from Sigma Aldrich (PA, USA). 1-(3-Dimethylaminopropyl)-3-ethylcarbodiimide Hydrochloride was purchased from TCI America (PA, USA). Phosphate Buffered Saline, sodium chloride, and bovine Albumin Serum were purchased from Fisher Scientific (PA, USA). Progesterone was purchased from Cayman Chemical Company (MI, USA). Progesterone x-aptamers were selected using the AM Biotechnologies X-Aptamer kit and were synthesized by AM Biotech. Biotin-labeled interleukin 6 (IL-6) aptamers were purchased from base pair biotechnologies (TX, USA). Near-infrared streptavidin-coated quantum dots were purchased from life technologies (CA, USA).

### *V.2.2 X-aptamer Selection*

A library of X-aptamers, bound to synthetic micro beads, was provided by AM Biotech. Aptamer selection was carried out according to the protocol provided by AM Biotech. In addition to the negative selection suggested in the protocol (removal from the library of the aptamers that bind to streptavidin coated magnetic beads), a second negative selection was carried out to remove aptamers that bind to biotin. Streptavidin coated magnetic beads were mixed with the aptamer library, incubated for an hour and then were

removed (along with bound aptamers) using a magnetic stand. The remaining library was incubated with 100 $\mu$ M biotin for an hour and the biotin along with bound aptamers was pulled down through binding to streptavidin-coated beads. From the remainder of the aptamers in the library, primary selection of aptamers specifically binding to progesterone was performed by incubation of the library with biotinylated progesterone, followed by harvesting of the biotinylated progesterone along with bound aptamers using streptavidin coated magnetic beads. These harvested aptamers were cleaved from the synthetic micro beads using 1N NaOH. This pool of selected aptamers was divided into three aliquots. One aliquot was incubated with streptavidin coated magnetic particles. Aptamers bound to these beads were pulled down along with the magnetic particles. This fraction (fraction #1) represents aptamers that bind to streptavidin and magnetic beads. Second aliquot was incubated with biotinylated progesterone. The bound aptamers were pulled down along with biotinylated progesterone through binding to streptavidin-coated beads. This is the fraction containing progesterone-binding aptamers (fraction #2). The third fraction was used as a representative pool of all aptamers selected in the primary selection. All three fractions were PCR amplified with specific reverse primer for each fraction. The PCR products were combined and used as template for next generation sequencing. From the sequences identified, those that were enriched in the fraction#2 were chosen as the sequences specific to progesterone binding aptamers. Finally, AM Biotech synthesized the 9 x-aptamers selected using the kit.

### *V.2.3 Sensor Chip Functionalization*

A bare gold sensor chip was cleaned under sonication using a nanostrip solution (50 °C, 90 mins) followed by thorough rinsing with ultrapure water. Then the sensor chip was placed in the UV/Ozone for 10 mins prior to surface functionalization. The first functionalization step with a layer of 11-MUA (34 mM in pure ethanol) was facilitated by microwave irradiation using a CEM discover microwave (50W, 50°C, 5 mins). The carboxyl groups of 11-MUA were activated by EDC first (65 mM in ultrapure water) in the microwave (50W, 50°C, 5 mins) and this was followed by reacting the surface with NHS (40 mM in ultrapure water) under the same conditions. Finally, PEG800 (1.25 mM in ultrapure water) is reacted with the sensor chip under the same microwave conditions. It is important to note that the sensor chip was washed thoroughly with ultrapure water between each functionalization step to ensure removal of unreacted chemicals. The chip was then dried with a stream of nitrogen and allowed to react with extravidin (0.2 mg/mL, 10 mM PBS) at room temperature and a relative humidity of 75% for 1 hour. After this step, the avidin chip was prepared for the ligand immobilization step by a thorough rinse with ultrapure water and dried with a stream of nitrogen.

### *V.2.4 Ligand Immobilization*

The avidin sensor chip was spotted with the biotin-labeled library of progesterone x-aptamers and negative interleukin 6 aptamer. In the direct detection-sensing assay, the spotting concentration of both positive progesterone and the negative control IL-6 aptamers was 100  $\mu$ M and prepared in a phosphate spotting buffer (10mM PBS, 10% glycerol, PH=7.4) solution. In the sandwich amplification-sensing assay, the optimal

spotting concentration of both positive progesterone and negative control IL-6 aptamers was 5  $\mu\text{M}$  and prepared in phosphate spotting buffer (10mM PBS, 10% glycerol, PH=7.4). The spotting was performed using LabNext compact Microarrayer and 300  $\mu\text{m}$  teflon spotting pin. The biotin-labeled x-aptamers were allowed to react with the avidin surface at room temperature and a relative humidity of 75% for 2 hours.

#### *V.2.5 NanoEnhanced Binding Assay*

The sensor surface was inserted into the SPRi instrument for assay analysis and a phosphate buffer (10 mM PBS, 4% Acetonitrile, PH=7.4) buffer was degassed and allowed to flow above the surface at room temperature and a flow rate of 5  $\mu\text{L}/\text{min}$ . Further blocking of the sensing surface was performed inside the instrument by sequentially injecting a BSA solution (1%) followed by a PEG2000 solution (1 mM) and the non-bound molecules were washed properly from the surface between steps. A calibration step using a solution of sucrose (3 mg/mL, 10 mM PBS PH=7.4, 4% Acetonitrile) was then performed and that precedes the injection of the analyte. The samples injected were diluted in the running buffer and loaded to a 150  $\mu\text{L}$  injection loop. In the direct detection-sensing assay, a solution of progesterone prepared in a 10 mM PBS and 4% acetonitrile solution was injected and the kinetics of the binding event were monitored. And in the sandwich amplification-sensing assay, the primary injection consisted of a specific concentration of progesterone sample followed 5 minutes after by the second injection consisting of a progesterone detection aptamer (x-aptamer #4) conjugated to the quantum dots. The signal amplification sample consisting of the detection aptamer (20 nM) was allowed to incubate with the streptavidin conjugated

quantum dots (10 nM) for 30 mins prior to injection above the sensing surface. And the kinetics of both steps was monitored in real-time. Finally, the SPRi sensorgrams were analyzed and the final plots were prepared using the ScrubberGen horiba software.

### **V.3 Results**

#### *V.3.1 Screening of Developed X-aptamers*

The biosensing assay was designed to achieve high specificity and selectivity for the detection of low progesterone titers down to 0.315 ng/mL levels. Specific aptamers were selected and employed as the surface ligands. Taking advantage of the strong bond between biotin and avidin, the aptamers were tagged with a biotin molecule; an avidin surface was employed for the direct attachment of the capture aptamer ligands to the sensing surface in a well-oriented manner. PEG800 was microwaved on the surface prior to the ligand immobilization since microwave irradiation of PEG-SH has been shown by a previous study to improve the effectiveness of the blocking process resulting in an enhanced SPRi response [89]. BSA (1%) and PEG2000 (1 mM) were further added to the surface inside the instrument to further block the sensing platform from non-specific adsorption of analyte. Long chain thiolated PEG offers the hydrophilic behavior that repels analyte molecules from binding non-specifically to the surface. The aptamers developed were screened for the detection of progesterone in the buffer (4% Acetonitrile, 10 mM PBS) used to solubilize progesterone. Progesterone is highly hydrophobic; hence, acetonitrile was utilized to solubilize the steroid and enable its detection in a water-based buffer (10 mM PBS). The performance of each aptamer is presented in Fig. 5.1 in which the 9 aptamers evoked different SPRi signals after the injection of 50 µg/mL (150 µM) of

progesterone. As shown, x-aptamers 3, 5 and 4 resulted in the highest SPRi response ( $\% \Delta R = 0.4 \pm 0.01$ ) upon the interaction with progesterone (150  $\mu\text{M}$ ); meanwhile, other x-aptamers experienced a lower binding response especially x-aptamer 1 which showed similar SPRi signal to the IL-6 negative control.

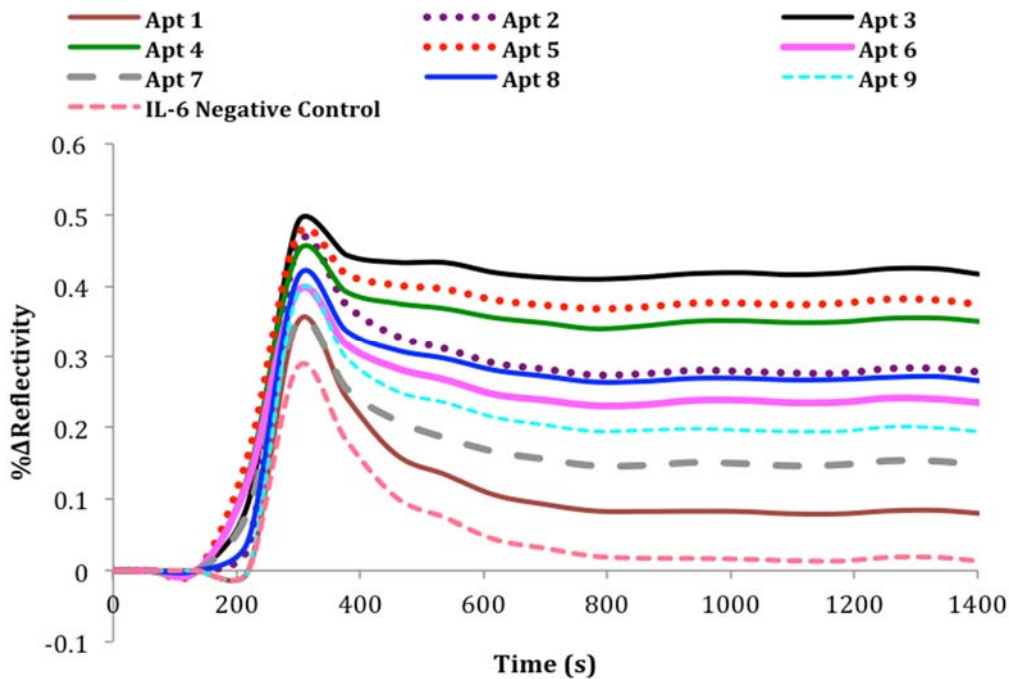


**Figure 5.1. Screening of All X-aptamers Using SPRi-based Direct Sensing. The SPRi sensorgrams of the interaction between progesterone (150  $\mu$ M) and the 9 x-Aptamers developed and the negative IL-6 control aptamer spotted at 100  $\mu$ M concentrations.**

### *V.3.2 Direct Detection Assay Measurements*

With the biosensing assay we were able to select several high binding activity aptamers from the library of aptamers developed that detected progesterone at a concentration of 49  $\mu$ g/mL (150  $\mu$ M). The next step was to test a range of concentrations (15.75, 31.5, 63, and 126  $\mu$ g/mL) of progesterone and monitor the SPRi response of the binding to one of the top aptamers (Aptamer #5), which produced the largest SPRi response ( $\% \Delta R$ ) upon interaction with progesterone. Aptamer 5 was spotted on the surface (N= 6 spots) along with the IL-6 aptamer (N=6 spots) as a negative control; the kinetic analysis was performed. A linear correlation was obtained by increasing the

concentration of progesterone injected to the functionalized surface and the results are presented in Fig. 5.2. As it can be shown, the limit of detection was concluded to be 15.75  $\mu\text{g/mL}$  (50  $\mu\text{M}$ ) resulting in a response of  $\% \Delta R = 0.07 \pm 0.01$  for the direct biosensing assay.

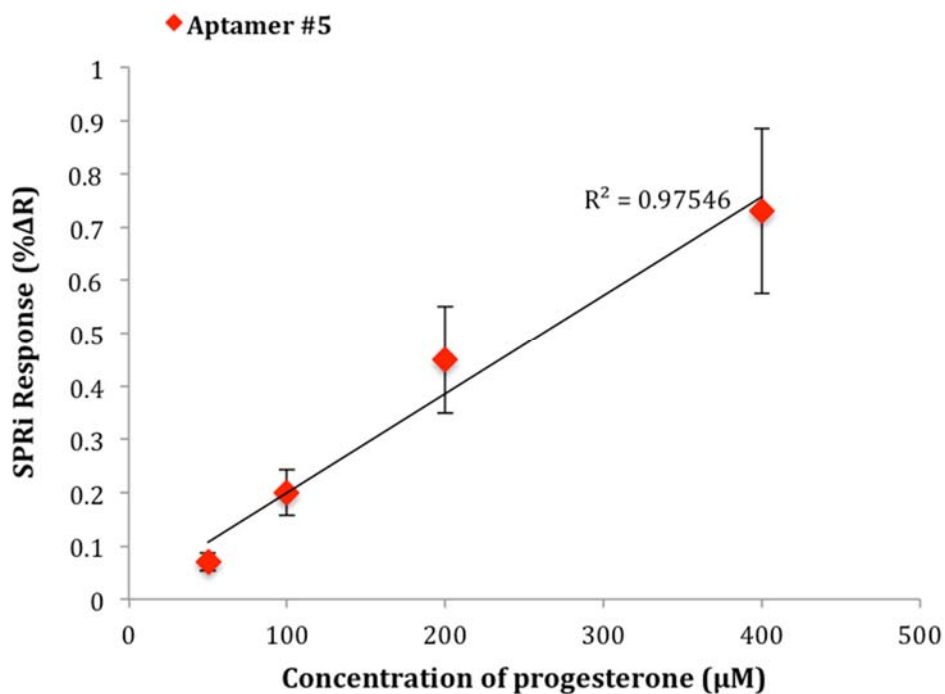


**Figure 5.2. A Direct Detection Concentration Profile of SPRi Response of Progesterone in Buffer. The SPRi signal is obtained from the interaction of x-aptamer #5 with progesterone in buffer at a concentration range (50-400  $\mu\text{M}$ ).**

### *V.3.3 Specificity Assay Measurements*

Aptamers are well known for their enhanced selectivity and specificity as minor structural differences between biomolecules can be distinguished through the recognition process [113]. Taking this potential property into account, we examined the specificity of

the positive aptamer (x-aptamer 5) by testing its detection against a closely related steroid,  $\beta$ -Estradiol (63  $\mu\text{g}/\text{mL}$ ) that coexists with progesterone in blood serum during the mid-menstrual cycle. The positive aptamer was chosen for further analysis due to its high binding SPRi signal shown in Fig. 2. The specificity assay was performed under the same conditions as the direct detection and utilized x-aptamer #5 with a solution containing  $\beta$ -Estradiol (63  $\mu\text{g}/\text{mL}$ ). As presented in Fig. 5.3, x-aptamer 5 showed significant specificity for only progesterone ( $\% \Delta R = 0.40 \pm 0.10$ ) and showed negligible binding to  $\beta$ -Estradiol.

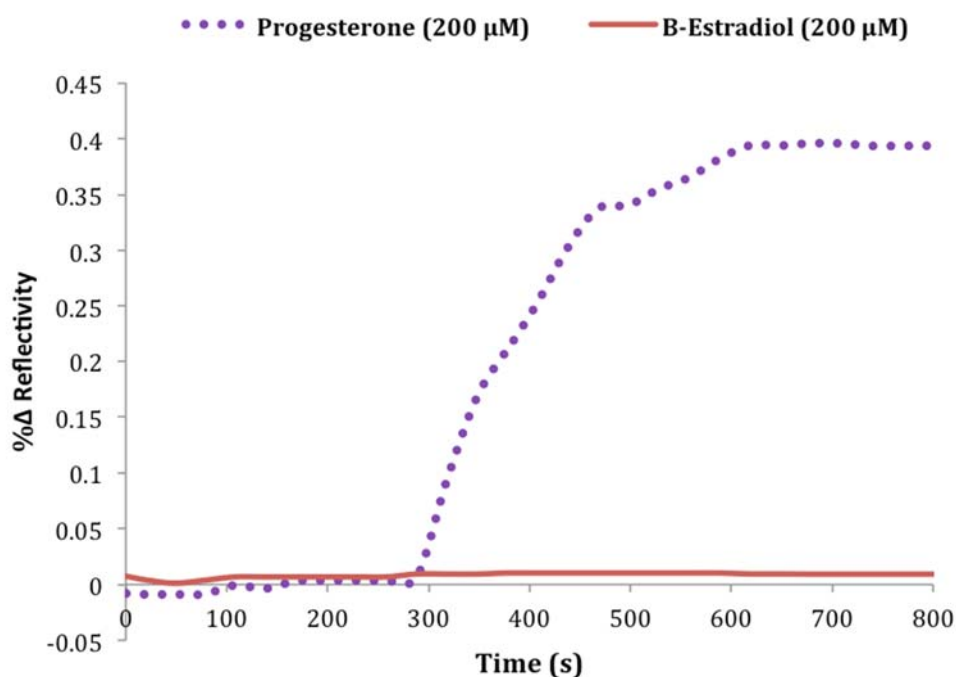


**Figure 5.3. A Specificity Assay Comparing the SPRi Response of Positive X-Aptamer 5 to Progesterone and  $\beta$ -estradiol. SPRi sensorgrams of the response obtained from the interaction of aptamer #5 with progesterone (purple dotted line) and  $\beta$ -estradiol (red solid line). Aptamer #5 demonstrated high-specificity as the SPRi signal obtained from the interaction with progesterone (63  $\mu\text{g}/\text{mL}$ ) is  $\% \Delta R = 0.40 \pm 0.10$  compared to a negligible signal after exposure to  $\beta$ -estradiol (63  $\mu\text{g}/\text{mL}$ ).**

#### *V.3.4 Sandwich-Amplification Assay*

On the diagnostic front, SPRi assays could have tremendous impact if the capability to perform small molecule sensing at ultra-low concentrations is successfully achieved. As previously mentioned, small molecule sensing is still in its early stage of development because of the problem posed by low molecular weight. In this work, we employed nanoenhancers (NIR quantum dots) as special signal amplification probes to generate a detectable signal at very low concentrations of progesterone. The sandwich

assay was carried out with a three-step procedure. First, progesterone was injected followed by a detection aptamer (x-aptamer #4). X-aptamer 4 was tested as a detection aptamer due to its high binding as shown in the screening assay (Figure 5.1). Finally the nanoenhancers were added to produce the SPRi signal enhancement.

A range of concentrations was examined in this setup to determine the lowest detection limit and thus, evaluate the sensitivity of the biosensing assay. The limit of detection was determined to be 0.315 ng/mL (1 nM). The concentration profile of the tested concentrations of progesterone is represented in Figure 5.4.

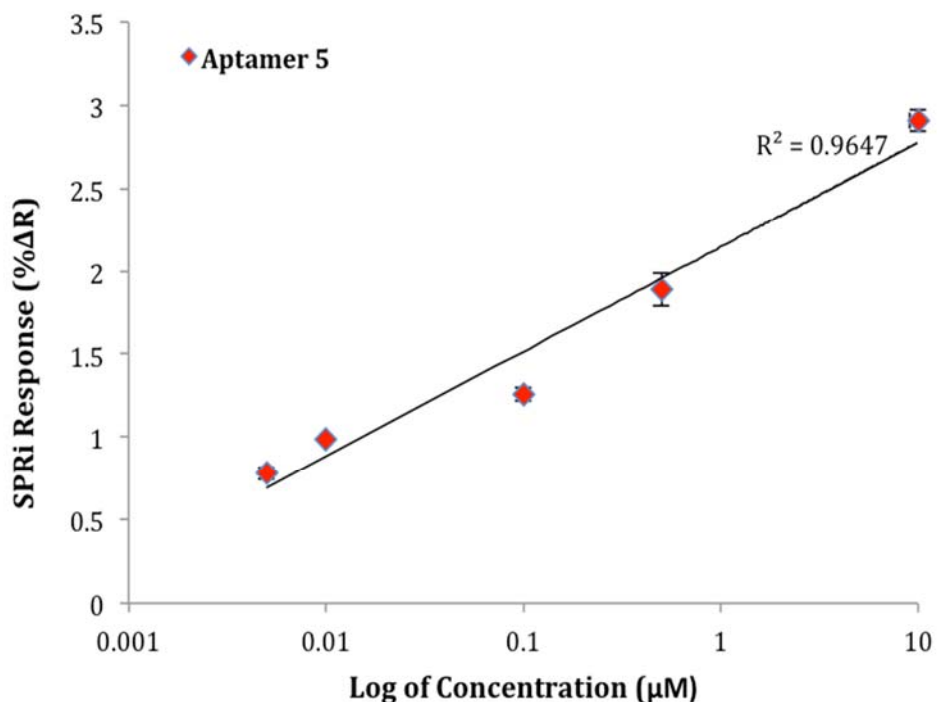


**Figure 5.4. A Sandwich-Amplification Assay Concentration Profile of Progesterone in Buffer. The SPRi response (%Δ Reflectivity) represents the interaction of nanoenhancers with the various amount of progesterone (0.005-10 μM) upon binding to x-aptamer #5.**

#### V.4 Conclusions

We developed specific x-aptamers for progesterone using an X-Aptamer kit because this approach offers an advantage over conventional aptamers as well as monoclonal antibodies in the selective and ultrasensitive detection of progesterone. X-aptamers are small single stranded DNA molecules that contain nucleotides with amino acid functional groups and other small molecules attached. These chemical modifications confer vast chemical diversity to the X-aptamers, allowing for increased specificity when binding to targets. This chemical diversity is made possible by the micro bead based and

non-PCR dependent selection process. In small molecule sensing, the accurate identification and detection of analyte necessitates highly sensitive capture ligands capable of efficiently binding to the analyte in solution in order to maximize the platform signal. Moreover, it requires that the capture ligands can discriminate between these structurally similar biomolecules that are present in the same complex samples.

Therefore, introducing progesterone x-aptamers in combination with the Nanoenhanced biosensing capabilities of SPRi offer many advantages over currently used SPR-based and non-SPR based immunosensing assays.

A validation of the binding capability of the x-aptamers was performed using the SPRi based assay. The screening of all x-aptamers was performed and x-aptamers (3, 4 &5) showed the highest SPRi response ( $\% \Delta$  Reflectivity) results. The SPRi response reflects the binding activity occurring on the surface; hence, the higher the response the higher the binding occurring between the analyte and immobilized ligand. Hence, x-aptamer #5 was chosen for the direct detection as well as the sandwich-amplification sensing assay.

This work describes the first SPRi setup to our knowledge to detect progesterone in a mobile phase through the interaction with specific aptamer ligands bound to the sensor surface. Meanwhile, other SPR-based studies achieved the measurement in an inhibition assay in which progesterone was covalently bound to the metal surface and mobile antibodies were flown over the surface [114, 115]. The presented sensor surface design consisted of immobilizing the progesterone x-aptamers on the surface. These progesterone aptamers were functionalized with a biotin reporter molecule at the 5' end of

the oligonucleotide since this would allow the aptamers to be immobilized on the sensing surface. The implemented modification in this assay offers the advantage of carrying out direct measurements of progesterone. It also eliminates any alterations to the structure of progesterone resulting from modifications required to attach the steroid to the sensor surface. Furthermore, the mobile phase was optimized to allow complete solubilizing of progesterone, which is inherently insoluble in phosphate buffer. We accomplished that step by using a mixture of acetonitrile (4%) and phosphate buffer (10 mM) as the preparation buffer of samples and running buffer.

The use of amplification probes was designated to reach lower limits of detection and it significantly improved the performance of the biosensing assay. A detection limit of 0.315 ng/mL (1 nM) may be deduced from the range of low concentrations tested. The NanoEnhancers responsible for the higher sensitivity in the platform are made of heavy metal nanoparticles (quantum dots) that result in a high SPRi response once added to the bound detection probes. Moreover, the NanoEnhancers could possibly display an energy coupling phenomenon with the oscillating surface plasmons on the metal surface as proposed by Malic *et al.* [55]. Therefore, both the mass loading effect and the energy-coupling phenomenon could be responsible for the enhancing effect the NanoEnhancers are demonstrating on the SPRi signal.

Label-free small molecule biosensing is a key area in the development of advanced diagnostic tools and analysis assays that can shed light on numerous biochemical processes. In this study, we developed a biosensing surface capable of performing analysis in a label-free and real time manner while demonstrating the ability

to ultra sensitively and selectively distinguish between similarly structured hormones.

And we anticipate that further investigation of the platform design can extend the diagnostic application to detect a variety of different steroids in complex matrices such as serum and saliva. Moreover, steroids can be detected simultaneously by employing a multiplex assembled sensor surface immobilized with highly specific x-aptamers.

## CHAPTER VI

### CONCLUSION AND FUTURE PERSPECTIVES

As a conclusion, ultrasensitive and selective measurement of different biomarkers was accomplished using a SPRi assay in combination with signal enhancers. The successful detection of hGH in serum at ultra-low concentrations using a monoclonal immunoassay has led to the development of a multiplex assay that assess disease biomarkers. The multi-target analysis required major improvements to the sensor design by altering the immobilization strategy of antibody ligands to the surface. SPRi in conjunction with signal amplification probes was further employed in the development of a highly selective steroid sensor that relies on x-aptamers as capture ligands. This bioassay not only achieved low limits of detection ( $> 1\text{nM}$ ), but also demonstrated high selectivity to only progesterone.

We anticipate that the analytical potential of SPRi will continue to provide insightful understanding to the interaction between different biomolecules in complex matrices. We also foresee tremendous impact on the medical diagnostic field as this optical assay reaches the lab-on-a chip point of care devices and carries out high throughput screening of an array of biological molecules.

Developments in instrumentation for a better resolution analysis are possible future trends of label-free analysis and merging advanced microfluidics to make the

detection highly reliable and efficient is another trend. Moreover, the detection of biomolecular interactions has begun and is expected to continue to merge with other analytical tools such as Mass Spectrometry, Raman Spectroscopy, Atomic Force Microscopy and many more to increase the efficacy of analysis of the bio-affinity of a variety of biomolecules. Improvements will also extend to cover further optimization to the sensor surface and ligand immobilization, which still requires better systematic strategies that lead to reproducible results. For this purpose, immobilization microarray spotting instruments exploited for ligand spotting will be further optimized for homogeneous spotted surfaces with little to no variability between density and biological activity of the different spotted ligands.

SPRi analysis is also emerging as a sensitive platform to the areas of cellular interactions and processes at the single cell level [17, 116-118]. This label-free tool overcomes the challenges posed by colorimetric assays that cannot discriminate between bulk cellular activity and single cell [119]. This is expected to combine with other techniques such as fluorescence [120] and Raman analysis to increase the understanding of cellular mechanisms and solve outstanding problems in the biomedical field. Therefore, the knowledge obtained of cellular analysis can be combined with biomarker analysis to provide a more comprehensive understanding of various disease processes and highlight possible therapeutic routes for treatment.

## REFERENCES

1. Makaraviciute, A. and A. Ramanaviciene, Site-directed antibody immobilization techniques for immunosensors. *Biosensors and Bioelectronics*, 2013. **50**: p. 460-471.
2. Huang, H.L., et al., Biomarker discovery in breast cancer serum using 2-D differential gel electrophoresis/ MALDI-TOF/TOF and data validation by routine clinical assays. *Electrophoresis*, 2006. **27**(8): p. 1641-50.
3. Baldwin, M.A., Mass spectrometers for the analysis of biomolecules. *Methods Enzymol*, 2005. **402**: p. 3-48.
4. Reyzer, M.L. and R.M. Caprioli, MALDI mass spectrometry for direct tissue analysis: a new tool for biomarker discovery. *J Proteome Res*, 2005. **4**(4): p. 1138-42.
5. Ruijter, J.M., et al., Evaluation of qPCR curve analysis methods for reliable biomarker discovery: bias, resolution, precision, and implications. *Methods*, 2013. **59**(1): p. 32-46.
6. Jain, K.K., *The Handbook of Biomarkers*. 2010: Humana Press.
7. Madeira, A., et al., Identification of protein-protein interactions by surface plasmon resonance followed by mass spectrometry. *Curr Protoc Protein Sci*, 2011. **Chapter 19**: p. Unit19 21.
8. Kim, M., et al., Surface plasmon resonance imaging analysis of protein-protein interactions using on-chip-expressed capture protein. *Analytical Biochemistry*, 2006. **351**(2): p. 298-304.
9. Oesterreicher, S., et al., Interaction of Insulin-like Growth Factor II (IGF-II) with Multiple Plasma Proteins: HIGH AFFINITY BINDING OF PLASMINOGEN TO IGF-II AND IGF-BINDING PROTEIN-3. *Journal of Biological Chemistry*, 2005. **280**(11): p. 9994-10000.
10. Vernon-Wilson, E.F., et al., CD47 is a ligand for rat macrophage membrane signal regulatory protein SIRP (OX41) and human SIRPalpha 1. *Eur J Immunol*, 2000. **30**(8): p. 2130-7.
11. Stockley, P.G. and B. Persson, Surface plasmon resonance assays of DNA-protein interactions. *Methods Mol Biol*, 2009. **543**: p. 653-69.
12. Vaidyanathan, V.G., L. Xu, and B.P. Cho, Binding kinetics of DNA-protein interaction using surface plasmon resonance. 2013.
13. Oh, B.K., et al., Surface plasmon resonance immunosensor for the detection of *Salmonella typhimurium*. *Biosens Bioelectron*, 2004. **19**(11): p. 1497-504.

14. Shankaran, D.R., K.V. Gobi, and N. Miura, *Recent advancements in surface plasmon resonance immunosensors for detection of small molecules of biomedical, food and environmental interest. Sensors and Actuators B: Chemical*, 2007. **121**(1): p. 158-177.
15. Watts, H.J., C.R. Lowe, and D.V. Pollard-Knight, *Optical Biosensor for Monitoring Microbial Cells. Analytical Chemistry*, 1994. **66**(15): p. 2465-2470.
16. Suraniti, E., et al., *Real-time detection of lymphocytes binding on an antibody chip using SPR imaging. Lab on a Chip*, 2007. **7**(9): p. 1206-1208.
17. Milgram, S., et al., *Antibody microarrays for label-free cell-based applications. Methods*, 2012. **56**(2): p. 326-33.
18. MacKenzie, C.R., T. Hiram, and J.T. Buckley, *Analysis of receptor binding by the channel-forming toxin aerolysin using surface plasmon resonance. The Journal of biological chemistry*, 1999. **274**(32): p. 22604-9.
19. Schasfoort, R.B.M. and A.J. Tudos. *Handbook of surface plasmon resonance*. 2008; Available, from:  
<http://public.eblib.com/choice/publicfullrecord.aspx?p=1185603>.
20. Ladd, J., et al., *Label-free detection of cancer biomarker candidates using surface plasmon resonance imaging. Anal Bioanal Chem*, 2009. **393**(4): p. 1157-63.
21. Lee, H.J., et al., *Fabricating RNA Microarrays with RNA–DNA Surface Ligation Chemistry. Analytical Chemistry*, 2005. **77**(23): p. 7832-7837.
22. Smith, E.A., et al., *Surface plasmon resonance imaging studies of protein-carbohydrate interactions. Journal of the American Chemical Society*, 2003. **125**(20): p. 6140-6148.
23. Li, Y., H.J. Lee, and R.M. Corn, *Detection of Protein Biomarkers using RNA Aptamer Microarrays and Enzymatically Amplified SPR Imaging. Analytical chemistry*, 2007. **79**(3): p. 1082-1088.
24. Peterson, A.W., R.J. Heaton, and R.M. Georgiadis, *The effect of surface probe density on DNA hybridization. Nucleic Acids Research*, 2001. **29**(24): p. 5163-5168.
25. Mannelli, I., et al., *DNA immobilisation procedures for surface plasmon resonance imaging (SPRI) based microarray systems. Biosensors and Bioelectronics*, 2007. **22**(6): p. 803-809.
26. Bassil, N., et al., *One hundred spots parallel monitoring of DNA interactions by SPR imaging of polymer-functionalized surfaces applied to the detection of cystic fibrosis mutations. Sensors & Actuators B: Chemical*, 2003. **94**(3).
27. Manera, M.G., et al., *Real-time monitoring of carbonarius DNA structured biochip by surface plasmon resonance imaging. J Opt A Pure Appl Opt Journal of Optics A: Pure and Applied Optics*, 2008. **10**(6).
28. Liu, W., Y. Chen, and M. Yan, *Surface plasmon resonance imaging of limited glycoprotein samples. Analyst*, 2008. **133**(9): p. 1268-73.
29. Song, F., et al., *Detection of oligonucleotide hybridization at femtomolar level and sequence-specific gene analysis of the Arabidopsis thaliana leaf extract with*

- an ultrasensitive surface plasmon resonance spectrometer. *Nucleic acids research*, 2002. **30**(14).
30. Li, Y., et al., Surface plasmon resonance immunosensor for IgE analysis using two types of anti-IgE antibodies with different active recognition sites. *Anal Sci*, 2007. **23**(1): p. 31-8.
  31. Li, Y., et al., Surface plasmon resonance immunosensor for histamine based on an indirect competitive immunoreaction. *Anal Chim Acta*, 2006. **576**(1): p. 77-83.
  32. Fischer, M.J., Amine coupling through EDC/NHS: a practical approach. *Methods Mol Biol*, 2010. **627**: p. 55-73.
  33. Ladd, J., et al., Label-free detection of cancer biomarker candidates using surface plasmon resonance imaging. *Analytical and bioanalytical chemistry*, 2009. **393**(4): p. 1157-63.
  34. Kallwass, H.K.W., et al., Site-specific immobilization of an L-lactate dehydrogenase via an engineered surface cysteine residue. *Biotechnol Lett Biotechnology Letters*, 1993. **15**(1): p. 29-34.
  35. Lee, J.M., et al., Direct immobilization of protein g variants with various numbers of cysteine residues on a gold surface. *Anal Chem*, 2007. **79**(7): p. 2680-7.
  36. Oh, K., et al., Rapid serodiagnosis with the use of surface plasmon resonance imaging for the detection of antibodies against major surface protein A of *Mycoplasma synoviae* in chickens. *Canadian Journal of Veterinary Research*, 2010. **74**(1): p. 71-74.
  37. Ro, H.-S., et al., Surface plasmon resonance imaging protein arrays for analysis of triple protein interactions of HPV, E6, E6AP, and p53. *PMIC PROTEOMICS*, 2006. **6**(7): p. 2108-2111.
  38. Tsai, W.-C. and I.-C. Li, SPR-based immunosensor for determining staphylococcal enterotoxin A. *Sensors and Actuators B: Chemical*, 2009. **136**(1): p. 8-12.
  39. Yang, C.Y., et al., Detection of picomolar levels of interleukin-8 in human saliva by SPR. *Lab Chip*, 2005. **5**(10): p. 1017-23.
  40. Piliarik, M., M. Bockov, and J. Homola, Surface plasmon resonance biosensor for parallelized detection of protein biomarkers in diluted blood plasma. *Biosensors and Bioelectronics Biosensors and Bioelectronics*, 2010. **26**(4): p. 1656-1661.
  41. Cao, C., et al., A strategy for sensitivity and specificity enhancements in prostate specific antigen-alpha1-antichymotrypsin detection based on surface plasmon resonance. *Biosens Bioelectron*, 2006. **21**(11): p. 2106-13.
  42. Krishnan, S., et al., Attomolar detection of a cancer biomarker protein in serum by surface plasmon resonance using superparamagnetic particle labels. *Angew Chem Int Ed Engl*, 2011. **50**(5): p. 1175-8.
  43. Meyer, M., M. Hartmann, and M. Keusgen, SPR-based immunosensor for the CRP detection A new method to detect a well known protein. *Biosensors and Bioelectronics Biosensors and Bioelectronics*, 2006. **21**(10): p. 1987-1990.

44. Corne, C., et al., *SPR-imaging based assays on an oligonucleotide-array to analyze DNA lesions recognition and excision by repair proteins. Nucleic Acids Symposium Series*, 2008. **52**(1): p. 249-250.
45. Feriotto, G., et al., *Biosensor technology and surface plasmon resonance for real-time detection of genetically modified Roundup Ready soybean gene sequences. J Agric Food Chem*, 2002. **50**(5): p. 955-62.
46. Lecaruyer, P., et al., *Surface plasmon resonance imaging as a multidimensional surface characterization instrument--application to biochip genotyping. Anal Chim Acta*, 2006. **573-574**: p. 333-40.
47. Chardin, H., et al., *Surface Plasmon Resonance imaging: a method to measure the affinity of the antibodies in allergy diagnosis. Journal of immunological methods*, 2014. **405**: p. 23-8.
48. Rebe Raz, S., et al., *Label-free and multiplex detection of antibiotic residues in milk using imaging surface plasmon resonance-based immunosensor. Analytical chemistry*, 2009. **81**(18): p. 7743-9.
49. Hu, W., et al., *Sensitive detection of multiple mycotoxins by SPRi with gold nanoparticles as signal amplification tags. Journal of Colloid And Interface Science*, 2014. **431**: p. 71-76.
50. Kwon, M.J., et al., *Nanoparticle-enhanced surface plasmon resonance detection of proteins at attomolar concentrations: comparing different nanoparticle shapes and sizes. Analytical chemistry*, 2012. **84**(3): p. 1702-7.
51. Kawaguchi, T., et al., *Surface plasmon resonance immunosensor using Au nanoparticle for detection of TNT. Sensors and Actuators B: Chemical Sensors and Actuators B: Chemical*, 2008. **133**(2): p. 467-472.
52. Lyon, L.A., M.D. Musick, and M.J. Natan, *Colloidal Au-enhanced surface plasmon resonance immunosensing. Analytical chemistry*, 1998. **70**(24): p. 5177-83.
53. Soelberg, S.D., et al., *Surface plasmon resonance detection using antibody-linked magnetic nanoparticles for analyte capture, purification, concentration, and signal amplification. Analytical chemistry*, 2009. **81**(6): p. 2357-63.
54. Foudeh, A.M., et al., *Sub-femtomole detection of 16s rRNA from Legionella pneumophila using surface plasmon resonance imaging. Biosensors and Bioelectronics Biosensors and Bioelectronics*, 2014. **52**(11): p. 129-135.
55. Malic, L., M.G. Sandros, and M. Tabrizian, *Designed biointerface using near-infrared quantum dots for ultrasensitive surface plasmon resonance imaging biosensors. Anal. Chem.*, 2011. **83**(13): p. 5222-9.
56. Popii, V. and G. Baumann, *Laboratory measurement of growth hormone. Clinica Chimica Acta*, 2004. **350**(1-2): p. 1-16.
57. Higham, C.E. and P.J. Trainer, *Growth hormone excess and the development of growth hormone receptor antagonists. Exp Physiol*, 2008. **93**(11): p. 1157-1169.
58. Sönksen, P., F. Salomon, and R. Cuneo, *Metabolic effects of hypopituitarism and acromegaly. Horm Res*, 1991. **36**(Suppl 1): p. 27-31.

59. Molitch, M., et al., Evaluation and Treatment of Adult Growth Hormone Deficiency: An Endocrine Society Clinical Practice Guideline. *J Clin Endocrinol Metab*, 2006. **91**(5): p. 1621-1634.
60. World Anti-Doping Agency. *The World Anti-Doping Code: The 2015 Prohibited List International Standard 2015*.
61. Agency, W.A.-D. *The 2014 prohibited list world anti-doping code 2014*. DOI: <https://wada-main-prod.s3.amazonaws.com/resources/files/WADA-Revised-2014-Prohibited-List-EN.PDF>.
62. Langkamp, M., K. Weber, and M.B. Ranke, Human growth hormone measurement by means of a sensitive ELISA of whole blood spots on filter paper. *Growth Horm IGF Res*, 2008. **18**(6): p. 526-532.
63. Rich, R.L. and D.G. Myszka, Survey of the year 2007 commercial optical biosensor literature. *J Mol Recognit*, 2008. **21**(6): p. 355-400.
64. Homola, J., Present and future of surface plasmon resonance biosensors. *Anal Bioanal Chem*, 2003. **377**(3): p. 528-539.
65. Hoa, X.D., A.G. Kirk, and M. Tabrizian, Toward Integrated Surface Plasmon Resonance Biosensors: A Review of Recent Progress. *Biosens Bioelectron*, 2007. **23**(2): p. 151-160.
66. de Juan-Franco, E., et al., Implementation of a SPR immunosensor for the simultaneous detection of the 22K and 20K hGH isoforms in human serum samples. *Talanta*, 2013. **114**(0): p. 268-275.
67. de Juan-Franco, E., et al., Site-directed antibody immobilization using a protein A-gold binding domain fusion protein for enhanced SPR immunosensing. *Analyst*, 2013. **138**(7): p. 2023-2031.
68. Du, H., et al., Immunological screening and characterization of highly specific monoclonal antibodies against 20 kDa hGH. *Bioanalysis*, 2012. **4**(17): p. 2161-2168.
69. Treviño, J., et al., Surface plasmon resonance immunoassay analysis of pituitary hormones in urine and serum samples. *Clin Chim Acta*, 2009. **403**(1-2): p. 56-62.
70. Wu, Z., et al., Detection of doping with human growth hormone. *Lancet*, 1999. **353**(9156): p. 895.
71. Vance, S.A. and M.G. Sandros, Zeptomole Detection of C-Reactive Protein in Serum by a Nanoparticle Amplified Surface Plasmon Resonance Imaging Aptasensor. *Sci. Rep.*, 2014. **4**(5129): p. 1-7.
72. Uludag, Y. and I.E. Tohill, Cancer biomarker detection in serum samples using surface plasmon resonance and quartz crystal microbalance sensors with nanoparticle signal amplification. *Anal. Chem.*, 2012. **84**(14): p. 5898-5904.
73. Špringer, T. and J. Homola, Biofunctionalized gold nanoparticles for SPR-biosensor-based detection of CEA in blood plasma. *Anal. Bioanal. Chem.*, 2012. **404**(10): p. 2869-2875.
74. Bartels, K., et al., Perioperative Organ Injury. *Anesthesiology*, 2013. **119**(6): p. 1474-1489.

75. Ebrahimkhani, M.R., et al., *Aag-initiated base excision repair promotes ischemia reperfusion injury in liver, brain, and kidney. Proc. Natl. Acad. Sci. U.S.A.*, 2014. **111**(45): p. E4878-86.
76. Brusniak, M.Y., et al., *An assessment of current bioinformatic solutions for analyzing LC-MS data acquired by selected reaction monitoring technology. Proteomics*, 2012. **12**(8): p. 1176-84.
77. Vaidya, V.S., M.A. Ferguson, and J.V. Bonventre, *Biomarkers of Acute Kidney Injury. Annu. Rev. Pharmacool. Toxicol.*, 2008. **48**: p. 463-493.
78. Garcia, E.P., et al., *Scalable Transcriptional Analysis Routine Multiplexed Quantitative Real-Time Polymerase Chain Reaction Platform for Gene Expression Analysis and Molecular Diagnostics. J Mol Diagn*, 2005. **7**(4): p. 444-454.
79. Öhrmalm, C., et al., *Variation-Tolerant Capture and Multiplex Detection of Nucleic Acids: Application to Detection of Microbes. J Clin Microbiol*, 2012. **50**(10): p. 3208-3215.
80. Rebe Raz, S., et al., *Label-free and multiplex detection of antibiotic residues in milk using imaging surface plasmon resonance-based immunosensor. Anal. Chem.*, 2009. **81**(18): p. 7743-9.
81. Lee, H.J., D. Nedelkov, and R.M. Corn, *Surface Plasmon Resonance Imaging Measurements of Antibody Arrays for the Multiplexed Detection of Low Molecular Weight Protein Biomarkers. Anal. Chem.*, 2006. **78**(18): p. 6504-6510.
82. Battaglia, T.M., et al., *Quantification of cytokines involved in wound healing using surface plasmon resonance. Anal. Chem.*, 2005. **77**(21): p. 7016-23.
83. Ladd, J., et al., *Label-free detection of cancer biomarker candidates using surface plasmon resonance imaging. Anal. Bioanal. Chem*, 2009. **393**(4): p. 1157-63.
84. Piliarik, M., M. Bockov, and J. Homola, *Surface plasmon resonance biosensor for parallelized detection of protein biomarkers in diluted blood plasma. Biosens. Bioelectron.*, 2010. **26**(4): p. 1656-1661.
85. Antoine, D.J., et al., *Mechanistic biomarkers provide early and sensitive detection of acetaminophen-induced acute liver injury at first presentation to hospital. Hepatology (Baltimore, Md.)*, 2013. **58**(2): p. 777-787.
86. Jaeschke, H., et al., *Mechanisms of hepatotoxicity. Toxicol. Sci*, 2002. **65**(2): p. 166-176.
87. Malhi, H. and G.J. Gores, *Cellular and molecular mechanisms of liver injury. Gastroenterology*, 2008. **134**(6): p. 1641-54.
88. Han, W.K., et al., *Kidney Injury Molecule-1 (KIM-1): a novel biomarker for human renal proximal tubule injury. Kidney Int.*, 2002. **62**(1): p. 237-44.
89. Vance, S.A. and M.G. Sandros, *Zeptomole Detection of C-Reactive Protein in Serum by a Nanoparticle Amplified Surface Plasmon Resonance Imaging Aptasensor. Sci. Rep.*, 2014. **4**: p. 5129.
90. Hahnefeld, C., S. Drewianka, and F.W. Herberg, *Determination of kinetic data using surface plasmon resonance biosensors. Methods Mol. Med.*, 2004. **94**: p. 299-320.

91. Jahanshahi, P., et al., *Rapid Immunoglobulin M-Based Dengue Diagnostic Test Using Surface Plasmon Resonance Biosensor*. *Sci. Rep.*, 2014. **4**: p. 3851.
92. Remy-Martin, F., et al., *Surface plasmon resonance imaging in arrays coupled with mass spectrometry (SUPRAMS): proof of concept of on-chip characterization of a potential breast cancer marker in human plasma*. *Anal. Bioanal. Chem*, 2012. **404**(2): p. 423-432.
93. de Juan-Franco, E., et al., *Site-directed antibody immobilization using a protein A-gold binding domain fusion protein for enhanced SPR immunosensing*. *Analyst*, 2013. **138**(7): p. 2023-31.
94. Mariani, S. and M. Minunni, *Surface plasmon resonance applications in clinical analysis*. *Anal. Bioanal. Chem.*, 2014. **406**(9-10): p. 9-10.
95. Chen, R., et al., *Emerging Role of High-Mobility Group Box 1 (HMGB1) in Liver Diseases*. *Mol. Med.*, 2013. **19**(1): p. 357-366.
96. Gaillard, C., et al., *A High-Sensitivity Method for Detection and Measurement of HMGB1 Protein Concentration by High-Affinity Binding to DNA Hemicatenanes*. *PLOS ONE*, 2008. **3**(8): p. e2855.
97. Yamada, S., et al., *High mobility group protein 1 (HMGB1) quantified by ELISA with a monoclonal antibody that does not cross-react with HMGB2*. *Clin. Chem.*, 2003. **49**(9): p. 1535-7.
98. Vaidya, V.S., et al., *A rapid urine test for early detection of kidney injury*. *Kidney Int.*, 2009. **76**(1): p. 108-14.
99. Wheeler, M.J. and J.S.M. Hutchinson. *Hormone assays in biological fluids*. 2006; Available from: <http://site.ebrary.com/id/10115223>.
100. Ehrentreich-Förster, E., F.W. Scheller, and F.F. Bier, *Detection of progesterone in whole blood samples*. *Biosensors and Bioelectronics*, 2003. **18**(4): p. 375-380.
101. Gillis, E.H., et al., *Improvements to a surface plasmon resonance-based immunoassay for the steroid hormone progesterone*. *Journal of AOAC International*, 2006. **89**(3).
102. Safronova, V.A., et al., *Lateral flow immunoassay for progesterone detection*. *Moscow Univ. Chem. Bull. Moscow University Chemistry Bulletin*, 2012. **67**(5): p. 241-248.
103. Ye, F., et al., *Competitive immunoassay of progesterone by microchip electrophoresis with chemiluminescence detection*. *Journal of Chromatography B*, 2013. **936**: p. 74-79.
104. Barnard, G., et al., *The measurement of progesterone in serum by a non-competitive idiometric assay*. *Steroids*, 1995. **60**(12): p. 824-9.
105. Gillis, E.H., et al., *Development and validation of a biosensor-based immunoassay for progesterone in bovine milk*. *Journal of Immunological Methods*, 2002. **267**(2): p. 131-138.
106. Wu, Y., et al., *Evaluation of progesterone-ovalbumin conjugates with different length linkers in enzyme-linked immunosorbant assay and surface plasmon resonance-based immunoassay*. *Steroids*, 2002. **67**(7): p. 565-572.

107. Yuan, J., et al., Sensitivity enhancement of SPR assay of progesterone based on mixed self-assembled monolayers using nanogold particles. *Biosensors and Bioelectronics*, 2007. **23**(1): p. 144-148.
108. Mitchell, J.S., et al., Sensitivity enhancement of surface plasmon resonance biosensing of small molecules. *Analytical Biochemistry*, 2005. **343**(1): p. 125-135.
109. Jayasena, S.D., Aptamers: an emerging class of molecules that rival antibodies in diagnostics. *Clinical chemistry*, 1999. **45**(9): p. 1628-50.
110. John, S.M. and W. Yinqiu, *Surface Plasmon Resonance Biosensors for Highly Sensitive Detection of Small Biomolecules*. 2010: INTECH Open Access Publisher.
111. Mascini, M., *Aptamers and their applications*. *Anal Bioanal Chem Analytical and Bioanalytical Chemistry*, 2008. **390**(4): p. 987-988.
112. Song, K.M., S. Lee, and C. Ban, *Aptamers and their biological applications*. *Sensors (Basel, Switzerland)*, 2012. **12**(1): p. 612-31.
113. Jayasena, S.D., *Aptamers: an emerging class of molecules that rival antibodies in diagnostics*. *Clin Chem*, 1999. **45**(9): p. 1628-50.
114. Wu, Y., et al., Evaluation of progesterone-ovalbumin conjugates with different length linkers in enzyme-linked immunosorbant assay and surface plasmon resonance-based immunoassay. *Steroids*, 2002. **67**(7): p. 565-72.
115. Mitchell, J.S., et al., Sensitivity enhancement of surface plasmon resonance biosensing of small molecules. *Anal Biochem*, 2005. **343**(1): p. 125-35.
116. Bombera, R., et al., DNA-directed capture of primary cells from a complex mixture and controlled orthogonal release monitored by SPR imaging. *Biosens Bioelectron*, 2012. **33**(1): p. 10-6.
117. Lee, S.H., H.J. Ko, and T.H. Park, Real-time monitoring of odorant-induced cellular reactions using surface plasmon resonance. *Biosens Bioelectron*, 2009. **25**(1): p. 55-60.
118. Yanase, Y., et al., *Surface plasmon resonance for cell-based clinical diagnosis*. *Sensors (Basel)*, 2014. **14**(3): p. 4948-59.
119. Zeidan, E., et al., *Surface plasmon resonance: a label-free tool for cellular analysis*. *Nanomedicine*, 2015. **10**(11): p. 1833-1846.
120. Chabot, V., et al., Identification of the molecular mechanisms in cellular processes that elicit a surface plasmon resonance (SPR) response using simultaneous surface plasmon-enhanced fluorescence (SPEF) microscopy. *Biosens Bioelectron*, 2013. **50**: p. 125-31.